Naval Research Laboratory

Stennis Space Center, MS 39529-5004

Results from Tests of Direct Wave Mixing in the Ocean's Surface Mixed Layer

PAUL J. MARTIN
ERICK ROGERS
RICK A. ALLARD
PATRICK J. HOGAN
JAMES G. RICHMAN

Ocean Dynamics and Prediction Branch
Oceanography Division

November 16, 2012

REPORT DOCUMENTATION PAGE

1. REPORT DATE *(DD-MM-YYYY)* 16-11-2012	2. REPORT TYPE Formal Report	3. DATES COVERED *(From - To)*

4. TITLE AND SUBTITLE

Results from Tests of Direct Wave Mixing in the Ocean's Surface Mixed Layer

5a. CONTRACT NUMBER

5b. GRANT NUMBER

5c. PROGRAM ELEMENT NUMBER
0602435N

6. AUTHOR(S)

Paul J. Martin, Erick Rogers, Rick A. Allard, Patrick J. Hogan, and James G. Richman

5d. PROJECT NUMBER

5e. TASK NUMBER

5f. WORK UNIT NUMBER
73-6288-02-5

7. PERFORMING ORGANIZATION NAME(S) AND ADDRESS(ES)

Naval Research Laboratory
Oceanography Division
Stennis Space Center, MS 39529-5004

8. PERFORMING ORGANIZATION REPORT NUMBER

NRL/FR/7320--12--10,216

9. SPONSORING / MONITORING AGENCY NAME(S) AND ADDRESS(ES)

Office of Naval Research
1 Liberty Center
875 N. Randolph Street, Suite 1425
Arlington, VA 22203-1995

10. SPONSOR / MONITOR'S ACRONYM(S)
ONR

11. SPONSOR / MONITOR'S REPORT NUMBER(S)

12. DISTRIBUTION / AVAILABILITY STATEMENT

Approved for public release; distribution is unlimited.

13. SUPPLEMENTARY NOTES

14. ABSTRACT

The parameterization of direct wave mixing proposed by Qiao et al. (2004) was tested with data from the Ocean Weathership Station (OWS) Papa in the northeast Pacific and with data from three NOAA buoys, two in the northeast Pacific and one in the northwest Atlantic. Previous testing has indicated that the commonly used Mellor-Yamada-type mixed-layer models tend to underpredict the mixed-layer depth (MLD) in the open ocean. Adding the vertical mixing proposed by Qiao et al. (2004) to the vertical mixing predicted by the Mellor-Yamada Level 2 turbulence model increased the predicted MLD and improved the agreement between the predicted and observed sea-surface temperature (SST) at Papa. However, the results of the tests showed two significant problems with the parameterization of the wave mixing. At OWS Papa, the wave mixing caused too much diffusion of heat through the seasonal thermocline below the mixed layer, and too much diffusion of the thermocline itself. At the NOAA buoys and, less conclusively, at OWS Papa, the wave mixing inhibited the formation of shallow mixed layers and their associated SST spikes during periods of light winds due to the presence of swell.

15. SUBJECT TERMS

Ocean turbulence   Wave mixing   Mixed Layer   Ocean Weathership Station Papa   NOAA buoy data   Ocean modeling

16. SECURITY CLASSIFICATION OF:

a. REPORT	b. ABSTRACT	c. THIS PAGE
Unclassified	Unclassified	Unlimited

17. LIMITATION OF ABSTRACT
SAR

18. NUMBER OF PAGES
38

19a. NAME OF RESPONSIBLE PERSON
Paul Martin

19b. TELEPHONE NUMBER *(include area code)*
(228) 688-5447

Standard Form 298 (Rev. 8-98)
Prescribed by ANSI Std. Z39.18

CONTENTS

RESULTS FROM TESTS OF DIRECT WAVE MIXING IN THE OCEAN'S SURFACE MIXED LAYER

1. INTRODUCTION

Some recent papers have discussed the possible role of direct mixing by nonbreaking surface gravity waves in the upper ocean and have formulated and tested parameterizations of such mixing. Some motivations cited for this work are (1) a failure of some models of upper-ocean mixing to mix sufficiently deeply relative to observations (Qiao et al. 2004), (2) results from wave-tank experiments that indicate the occurrence of turbulent mixing during the passage of nonbreaking surface waves (Babanin 2006; Babanin and Haus 2009; Dai et al. 2010), and (3) the need for a physical mechanism to account for the observed attenuation of propagating swell (Babanin 2006). The purpose of this report is to test the direct wave mixing scheme proposed by Qiao et al. (2004) using time series of surface marine and upper-ocean observations from several locations.

Qiao et al. (2004) formulated an eddy coefficient mixing profile B_v computed from the surface wave spectrum as

$$B_v = \alpha \int_{\mathbf{k}} \int E(\mathbf{k}) \exp(2\mathbf{kz}) \mathbf{dk} \frac{\partial}{\partial \mathbf{z}} \left[\int_{\mathbf{k}} \int \omega^2 \mathbf{E}(\mathbf{k}) \exp(2\mathbf{kz}) \mathbf{dk} \right]^{\frac{1}{2}}, \qquad (1)$$

where α is a nondimensional scaling factor, E is the wave energy spectrum, k is the wave number, z is the vertical coordinate, and ω is the wave frequency. They tested the wave-mixing formulation in Eq. (1) with $\alpha = 1$ by computing upper-ocean mixing in a global domain from 75 °S to 65 °N using 6-h National Center for Environmental Prediction (NCEP) reanalysis wind fields to drive the Marine Science and Numerical Modeling (MASNUM) model, a coupled, ocean, wave-current model based on Yuan et al. (1999). Based on a minimum mixing rate of 5 cm^2/s, the wave mixing computed from Eq. (1) was found to provide mixing as deep as 90 m in the southern ocean.

Qiao et al. (2004) applied their wave-mixing model described by Eq. (1) to a climatological calculation of mixing in the global ocean from 75 °S to 65 °N using the Princeton Ocean Model (POM) (Blumberg and Mellor 1987), climatological wind stress and heat fluxes from the Comprehensive Ocean-Atmosphere Data Set (COADS), and temperature and salinity from the Levitus (1982) climatology. Mixing was computed using (a) just the Mellor-Yamada Level 2.5 (MYL2.5) turbulence model within POM, and (b) with the B_v wave mixing from Eq. (1) added to the momentum and scalar eddy-coefficient mixing profiles computed by the MYL2.5 turbulence model in POM. The two simulations were each run for six years. Qiao et al. (2004) reported that the simulation that included the B_v wave mixing produced temperature and salinity distributions in much better agreement with the Levitus climatology than the simulation without the wave mixing.

Babanin (2006) hypothesized that turbulence generated by nonbreaking surface waves would occur above a critical Reynolds number (computed from the orbital velocity of the waves and the

Manuscript approved December 16, 2011.

molecular viscosity of the water) of about 3000. In some preliminary testing of this hypothesis, Babanin (2006) found this value of the critical Reynolds number to be consistent with turbulence observed for mechanically generated waves in a laboratory wave tank and also roughly consistent with the surface waves and mixed-layer depth (MLD) occurring in the Black Sea in April 1986, at Ocean Weathership Stations (OWSs) November and Papa in April 1961, and for the April climatology of surface waves and MLD along 30 °N in the Atlantic and Pacific.

Babanin and Haus (2009) conducted experiments in a wave tank to investigate mixing within nonbreaking surface waves. They observed mixing occurring within the waves propagating along the length of the tank and intermittently measured velocity spectra consistent with the presence of isotropic turbulence below the waves. The occurrence of turbulence in the wave tank was determined to be roughly consistent with the Reynolds number cutoff of about 3000 proposed by Babanin (2006).

Babanin et al. (2009) tested wave mixing in the climate model CLIMBER-2 by replacing the fixed MLD of 50 m with a variable MLD based on the depth of direct wave mixing hypothesized by Babanin (2006). The waves were estimated from the wind field. Results were compared with the Naval Research Laboratory (NRL) global mixed-layer atlas (http://www7320.nrlssc.navy.mil/nmld/nmld.html). The version of CLIMBER-2 with a variable MLD computed from the wave mixing was found to give better results than the version with the fixed MLD of 50 m.

Dai et al. (2010) conducted experiments in a wave tank to investigate mixing within nonbreaking surface waves. A difference from Babanin and Haus (2009) is that the water was thermally stratified instead of being unstratified. They found that the water became well mixed within tens of minutes in the presence of waves, but took about 20 h to become well mixed without waves, and that the time required for the water to thermally mix decreased as the amplitude and wavelength of the waves were increased.

The evaluations of the wave mixing proposed by Qiao et al. (2004) and Babanin et al. (2009) for mixing in the upper ocean have mainly been done either with climatological data or using approximate, averaged values of forcing, waves, or MLD. The purpose of this report is to test the wave-mixing formulation of Qiao et al. (2004) given by Eq. (1) with real-time, time-series data, which should provide a more detailed comparison of the proposed wave-mixing with observations. Simulations were conducted at OWS Papa in the northeast Pacific, which has been a popular location for testing mixed-layer models (MLMs), and with data from the National Oceanic and Atmospheric Administration (NOAA) National Data Buoy Center (NDBC) buoys in the northeast Pacific and northwest Atlantic that include both surface marine observations, from which atmospheric forcing can be computed, and spectral wave observations, from which B_v wave-mixing profiles can be computed.

The following sections contain data and results from OWS Papa in the northeast Pacific (Section 2), data and results from NOAA Buoy 46005 in the northeast Pacific (Section 3), data and results from NOAA Buoy 46047 in the northeast Pacific (Section 4), data and results from NOAA Buoy 41049 in the Sargasso Sea (Section 5), and a summary (Section 6).

2. SIMULATION OF THE MIXED LAYER AT OCEAN STATION PAPA

OWS Papa was located in the northeast Pacific at 145 °W, 50 °N. The availability of long time series of meteorological and ocean subsurface measurements at Papa, and the fact that the effects of advection on the heat budget tend to be small in this area, have long made the data from Papa popular for testing and evaluating upper-ocean MLMs (Denman and Miyake 1973; Mellor and Durbin 1975; Martin 1985; Martin 1986; Gaspar 1988; Large et al. 1994; Kantha and Clayson 1994; Large 1996).

There are a number of issues involved with testing MLMs, even at as optimal a location as Papa, and since these can significantly affect the results of testing, some of them are discussed here.

2.1 Model

The model used to perform the simulations of the surface mixed layer (SML) described in this report is the Navy Coastal Ocean Model (NCOM) (Martin 2000; Morey et al. 2003; Barron et al. 2004). Though NCOM is a fully three-dimensional model, for this study, NCOM was run at a single location by using doubly periodic, lateral boundary conditions and the minimum, allowable horizontal grid (2 by 2 grid points). The vertical turbulence model that was used is the Mellor-Yamada Level 2 (MYL2) MLM (Mellor and Yamada 1974; Mellor and Durbin 1975; Martin 2000).

A uniformly stretched vertical grid of 40 layers was used with an upper-layer thickness of 1 m and a maximum depth of 5500 m. With this grid, each layer is 19% thicker than the layer above, and there are 21 layers in the upper 200 m. This is typical of the vertical grids used in regional simulations conducted with NCOM.

2.2 Heat Budget

The local, upper-ocean, heat budget is one of the most important aspects of testing MLMs, since even small biases in the mean surface heat flux have a cumulative effect on the upper-ocean thermal structure and significantly affect the MLD on time scales of more than a few days. At Papa, the surface heat fluxes are computed from 3-h surface marine observations of wind speed, air temperature and humidity, sea-surface temperature (SST), and cloud cover using standard air-sea flux formulas (Martin 1985). The heat fluxes computed using these formulas are probably uncertain within a factor of 20% or so.

A couple of considerations for the calculation of the surface heat flux at a location like Papa are (a) how well do the changes in the seasonal upper-ocean heat content predicted by the computed heat fluxes agree with the observed changes in heat content, and (b) how well does the surface heat flux balance over the year. For (a), if the SST, MLD, and isotherm depths (ISODs) of the model simulations all agree fairly well with the observations, then it might be considered that the surface heat fluxes being used are consistent with the observed changes in the upper-ocean thermal structure and that the MLM being used is doing a fairly good job of predicting the observed MLDs. For (b), if the net effects of advection on the heat budget over the year are small, then it would be expected that the mean surface heat flux over the year would be small. Of course, it is possible that the surface heat flux calculation being used is biased to some degree, or that part of the local, upper-ocean, heat budget is being made up by advection, or both.

Two scaling factors were used to adjust the levels of the surface heat flux used at Papa: F_r is used to scale the solar radiation, and F_e is used to scale the latent and sensible heat fluxes. The default values of these two scaling factors were taken to be $F_r = 0.94$ to account for the local albedo, i.e., the fraction of the incoming solar radiation that is reflected back into the atmosphere near the ocean's surface and is, therefore, not absorbed by the ocean is taken to be 6%, and $F_e = 1.0$, i.e., the latent and sensible heat fluxes (as well as the net longwave radiation) are used as computed by the bulk formulas. These default values of the heat-flux scaling parameters give a net surface heating at Papa of 17.7 W/m² for the year 1961.

2.3 Wind Stress

The surface wind stress at Papa was computed from the observed wind speed and direction using a standard bulk formula and the wind-speed-dependent drag coefficient of Garratt (1977). With this calculation of the surface wind stress and the calculation of the heat fluxes described in the previous section, a notable feature of many of the MLM simulations at Papa is the large SST peaks that are predicted during periods of very light winds. These SST peaks are frequently larger than those that are seen in the observations at Papa.

This allows for several possibilities: (a) the observed SST peaks during calm conditions are not fully captured by the observations, (b) the winds during calm periods are not as light as reported, or (c) some process is acting to mix the near-surface ocean water, even during calm conditions.

The SST peaks simulated by the MYL2 MLM used in this study are limited by the thickness of the uppermost layer used in the underlying numerical model, which was set to 1 m. A thinner upper-layer thickness would be capable of simulating shallower mixed layers and, hence, larger SST peaks. However, the fact that the SST peaks predicted here by NCOM at Papa are frequently larger than those that are observed suggests that an upper-layer thickness of 1 m for MLM simulations at Papa is generally adequate.

The SSTs observed at Papa during 1961 were measured in two ways: (a) by a bucket sample of the surface water, the temperature of which was measured with a thermometer to a precision of about 0.5 °C (which is similar to the precision of the air and dew point temperatures), and (b) by a mechanical bathythermograph (MBT), which is an instrument that is lowered on a cable and which inscribes the measured temperature on a coated glass slide. The temperature profiles were obtained by reading the temperature off the glass slide at intervals of 5 m after the MBT had been retrieved. For this study, the air-sea fluxes were computed using the bucket SST, and the SST from the MBTs is used in the SST plots since the MBT temperatures were recorded with more precision.

A question that arises is whether the light winds reported at Papa during near-calm conditions are lighter than actually occurred, i.e., perhaps the winds were too light to activate the anemometer. Is there a minimum wind speed that the anemometers can measure? We don't know the answer to this question. However, it has been suggested that a minimum effective wind speed to use for computing air-sea fluxes should be something like 2 m/s, and this minimum wind speed was used to compute the wind stress and heat flux values at Papa. Note that the wind stress for a 2 m/s wind speed is too small to prevent the formation of shallow mixed layers during periods of light winds by the MYL2 MLM.

Another possibility for the shortage of observed SST peaks during periods of calm winds is that there is a mixing process that can occur during calm wind conditions. Such a process is the proposed B_v wave mixing that is being investigated in this report. Babanin (2006), Babanin and Haus (2009), and Dai et al. (2010) report mixing occurring below propagating, nonbreaking waves in a laboratory tank. This laboratory situation is roughly analogous to that of swell occurring on the ocean's surface during calm conditions due to the propagation of waves from other areas. If surface waves can directly induce mixing, such swell might increase the mixing that occurs during calm wind conditions and reduce SST spikes.

2.4 Surface Moisture Flux

The moisture flux at the ocean's surface is due to evaporation and precipitation. These affect the salinity and, hence, the density stratification near the ocean's surface, since the loss (or gain) of water increases (or decreases) the salinity concentration near the surface. Evaporation can be estimated from the calculated latent heat flux. However, rainfall data at Papa are not generally available.

Since rainfall data at Papa for 1961 are not available, there are a couple of choices. One is just to ignore the surface moisture flux, i.e., set it to zero. This is frequently done in ocean mixed-layer simulations, since rainfall data are generally not available and changes in the near-surface density stratification due to the surface moisture flux tend to be small relative to the effects of the surface heat flux and tend to have only a small effect on the vertical mixing.

Another option is to relax the sea-surface salinity (SSS) to monthly climatological values if the seasonal variation of the SSS is significant. Such a relaxation is frequently used in large-scale ocean simulations.

Another option is to apportion an estimate (e.g., climatological) of the mean rainfall over those time periods when the near-surface humidity and cloud cover are high. Times when the humidity and cloud cover are near 100% frequently indicate that rainfall is occurring, but of course, this does not indicate how hard it is raining during a particular rain event.

For the simulations conducted here, the surface moisture flux was set to zero.

2.5 Solar Extinction

Jerlov (1968, 1976) categorized the solar extinction of "open" (i.e., not coastal) ocean waters using five different types, denoted, from the clearest to the most turbid, as Optical Type I, IA, IB, II, and III, and Jerlov and others have published maps of the regional distribution of these water types (Jerlov 1968; Rutkovskaya and Khalemskiy 1973; Jerlov 1976). The location of Papa was characterized by Rutkovskaya and Khalemskiy (1973) and Jerlov (1976) as moderately turbid Type II, and so this water type was used to define the solar extinction for the Papa simulations conducted for this report.

2.6 Background Diffusion

Vertical mixing below the turbulent SML is frequently parameterized by a small, constant, ambient or background level of mixing. An ambient diffusivity of 0.02 cm^2/s, as used at Papa by

Martin (1985), was used for the simulations conducted here for all the model fields, i.e., momentum, heat, and salinity.

Some test simulations were conducted at Papa with larger values for the ambient diffusivity to see what the effect would be. For a value of 0.1 cm^2/s, the predicted SST was reduced slightly and the depth of the SML and the ISODs were increased slightly during the summer due to more heat being diffused downward out of the SML. Larger values of the ambient diffusivity of 0.2 cm^2/s and higher resulted in further reduction of the predicted summer SST as more heat was diffused downward out of the SML. These larger values of the ambient diffusivity also resulted in reducing the sharpness of the seasonal thermocline below the SML. Since the seasonal thermocline at Papa is observed to be quite sharp (e.g., see the ISODs in Fig. 1), values of ambient diffusivity larger than 0.1 cm^2/s may not be desirable.

2.7 Ocean T and S Data

As previously mentioned, temperature profiles at Papa in 1961 were typically taken at 3-h time intervals with a MBT, with temperature values read from the glass slide from the MBT at intervals of 5 m. However, salinity profiles were not measured regularly. The measured temperature profiles were used to provide both initialization and validation of the mixed-layer simulations at Papa.

The mixed-layer simulations at Papa were initialized at 00Z on January 1, 1961 using the observed temperature profiles and a climatological salinity profile. An advantage of initializing mixed-layer simulations at this time of year is that the SML is near its deepest and, hence, the evolution of the upper-ocean thermal structure though the spring and summer is not very sensitive to the initial conditions, i.e., the development of the upper-ocean thermal structure in spring and summer starts with a "clean slate."

2.8 Results

2.8.1 Preliminary Testing at Papa

Figure 1 shows a simulation of the SML at Papa for 1961 using just the MYL2 MLM. In the figure, the results of the simulation (red) are compared with the observations (black).

As in Martin (1985, 1986), the SST is too high in summer and, consistent with this, the MLD and ISODs are too shallow. In Fig. 1, the summer SST is about 3 °C too high and the MLD and ISODs are 15 to 20 m too shallow in August and September. The situation in Fig. 1 is a bit worse than in Martin (1985, 1986) because, for this simulation, the surface heat flux has been set a bit higher to provide better agreement with the observed upper-ocean heat content at Papa in the summer.

A number of investigators have noted that the Mellor-Yamada-type turbulence models, e.g., the MYL2 (Mellor and Yamada 1974) and MYL2.5 (Mellor and Yamada 1982) models, frequently underpredict the observed depth of mixing in the open ocean (Martin 1985; Large et al. 1994; Kantha and Clayson 1994). However, this might be expected, since a number of processes that could contribute to increasing the vertical mixing, e.g., surface waves, Langmuir circulations, and internal waves, are not accounted for in these models.
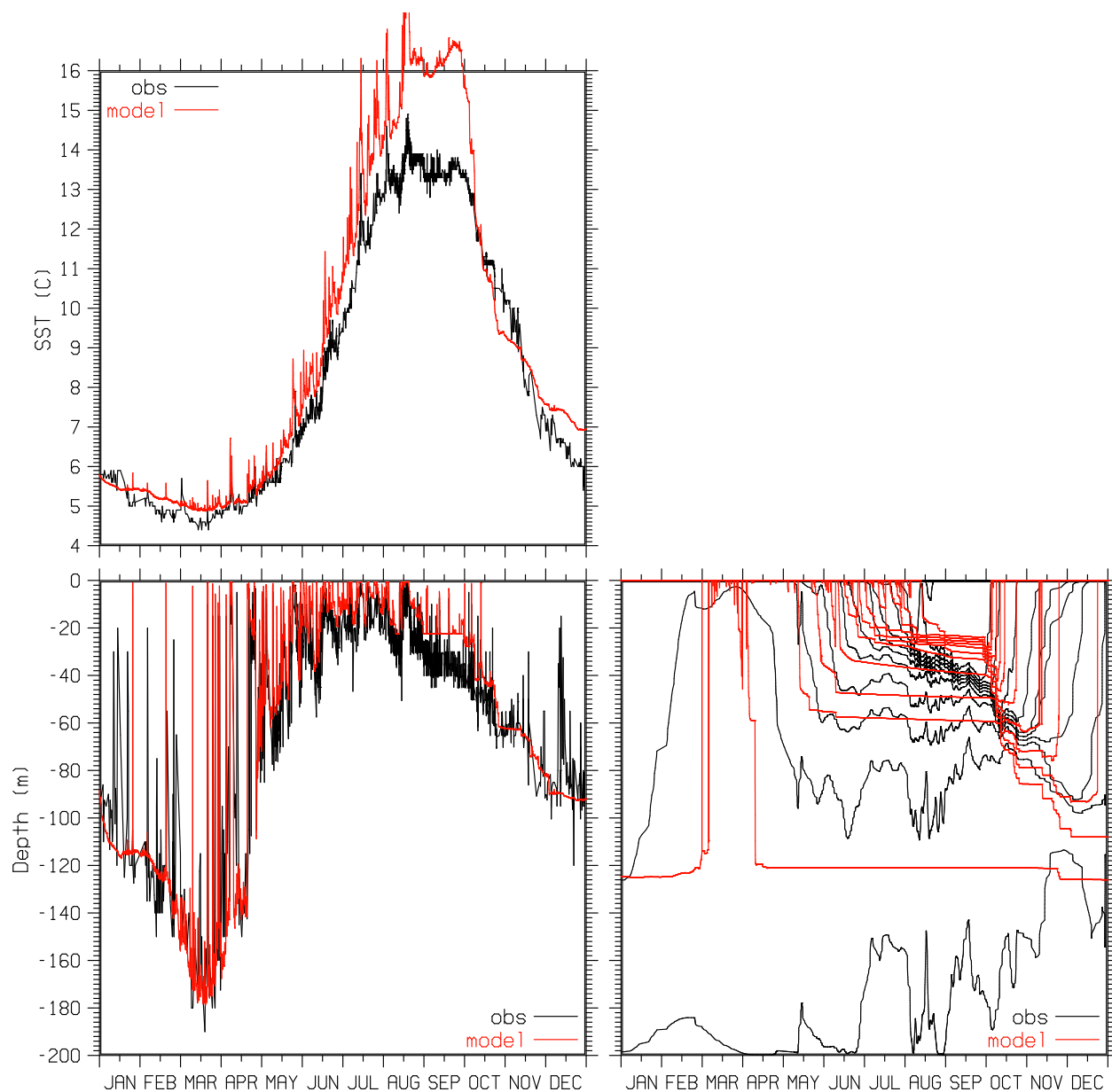
Fig. 1 — SST, MLD, and ISODs at OWS Papa for 1961: observed (black), simulated with MYL2 MLM (red)
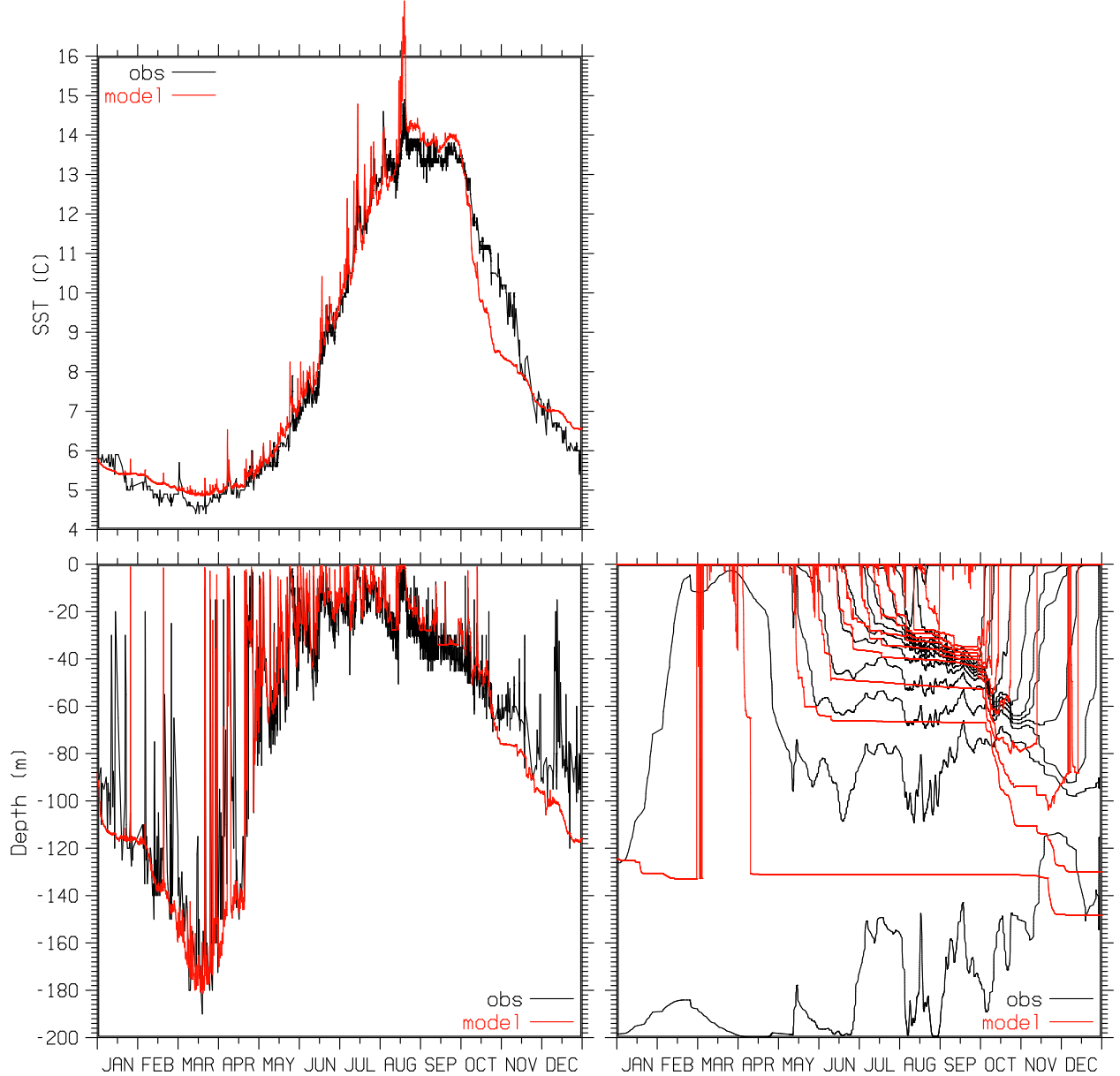
Fig. 2 — SST, MLD, and ISODs at OWS Papa for 1961: observed (black), simulated with MYL2 MLM
with Large et al. (1994) mixing enhancement (red)

A number of enhancements have been proposed over the years to increase the depth of mixing
of the Mellor-Yamada-type turbulence models. Figure 2 shows results from a simulation at Papa
for 1961 in which the MYL2 MLM has been modified to include the mixing enhancement of Large
et al. (1994; see also Kantha and Clayson 1994). This enhancement increases mixing above the
critical Richardson number of the MYL2 MLM of about 0.23 by adding a maximum mixing rate
of 50 cm^2/s at a Richardson number of zero, which decreases to zero at a Richardson number of
0.7. This enhancement is assumed to account for intermittent mixing processes near the base of
the SML, such as breaking internal waves.

Figure 2 shows significant improvement over the previous simulation in Fig. 1. The agreement
of the SST is fairly good during the spring, and is only about 0.4 °C too high in the summer.

Consistent with this, the MLD and ISODs are about 5 m too shallow in August and September. In the fall, in October and November, the model SST becomes lower and the MLD deeper than the observed values. It is thought that this discrepancy, which has occurred with a number of different MLMs used to simulate the mixed layer at Papa (Martin 1985; Martin 1986) is due to advection (Large 1996).

One noticeable difference between the model-simulated and observed SST in Fig. 2 is that many of the simulated SST peaks, which occur during periods of light winds, are larger than the observed peaks. This is in spite of the 2 m/s minimum wind speed used to compute the wind stress and heat fluxes that are used to drive the model. This discrepancy may be due to the simulated peaks being too large, or the observed peaks being smaller than those that actually occurred, or some of both.

There are fairly strong internal tides and internal waves at Papa, which add a significant short-time-scale variability to the observed MLD and ISODs (Davis et al. 1981), e.g., Levine et al. (1983) cite the vertical displacement of the M_2 internal tide to be about 10 m. The observed MLD in the figures is not filtered in time; hence, it is expected that the deep envelope of the observed MLD will exceed that of the simulated MLD when the MLD is simulated correctly except for the neglect of internal tides and waves. However, the high degree of variability of the observed ISODs due to the internal tides, internal waves, and other short-time-scale processes necessitates fairly strong temporal filtering to render the plots of the observed ISODs legible.

The fact that the simulated SST, MLD, and ISODs in Fig. 2 are all fairly close to the observed values in the spring and summer suggests that the net surface heat flux used for this simulation during this time is close to being correct, i.e., the amount of heat being added to the upper ocean during the spring and summer from the surface heat fluxes is fairly consistent with what is observed. This is consistent with the analysis of the heat budget at Papa by Large (1996), who reported that the net surface heat flux tended to balance the local, upper-ocean, heat content at Papa fairly well in the spring and summer. The ISODs in Fig. 2 show that the simulation does a good job of preserving the very sharp thermocline below the SML in the summer and early fall.

2.8.2 Testing the Direct Wave Mixing of Qiao et al. (2004) at Papa

To allow calculation of the B_v wave-mixing profiles of Qiao et al. (2004) for Papa for 1961, the SWAN wave model was run using the observed winds from Papa, and the B_v profiles were computed from the SWAN spectral wave output using Eq. (1). The value of the scaling factor α in Eq. (1) was set to one as it was for the simulations conducted by Qiao et al. (2004). Similar to Qiao et al. (2004), these B_v profiles were added to the eddy-coefficient profiles computed by the MYL2 MLM. In this case, the Large et al. (1994) mixing enhancement was not used, as it was considered that the B_v wave mixing might provide sufficient additional mixing.

Running a wave model like SWAN at a single location involves some approximations and uncertainties. An obvious problem is that wave propagation from other areas cannot properly be accounted for. This is especially significant when the local winds and the associated local wind-sea die and the largest contribution to the local waves is from swell propagating from other areas. When SWAN is run at a single location, the assumption is that the winds and associated waves are the same everywhere. Hence, swell that remains after the winds have died is the swell that was

generated from the local waves when the wind was blowing. How long this swell persists depends on the dissipation used in the wave model. For the SWAN simulations conducted at Papa, the dissipation scheme used is the "$n = 2$" scheme discussed in Rogers et al. (2003), which gave good results for most of the wave simulations they evaluated. Note that this scheme results in less dissipation of low-frequency waves than some of the other dissipation schemes that have been used in SWAN. The uncertainties in the SWAN-predicted wave propagation and dissipation must be kept in mind when considering the results of the wave mixing at Papa.

A question is whether the Reynolds number cutoff value of 3000 hypothesized by Babanin (2006) for the the direct wave mixing would affect the mixed-layer simulations. For deep-water surface waves, the value of B_v can be related to the wave Reynolds number R_e by

$$B_v = (\frac{k^3}{g})^{\frac{1}{4}}(\frac{\mu R_e}{2})^{\frac{3}{2}}, \tag{2}$$

where g is the acceleration of gravity and μ is the molecular viscosity of seawater. For typical wavelengths of 50 to 200 m, Eq. (2) gives B_v values of 0.04 to 0.11 cm^2/s. A simulation at Papa with a B_v cutoff of 0.1 cm^2/s, i.e., with B_v values below 0.1 cm^2/s set to zero, showed no noticeable difference from a simulation conducted without the cutoff being employed. Hence, it was determined that employing a cutoff Reynolds number of 3000 for the Qiao et al. (2004) parameterization of direct wave mixing in the ocean's surface layer would not significantly affect the results.

Figure 3 shows results from the simulation at Papa with the B_v wave mixing added to the mixing from the MYL2 MLM. The agreement of the simulated and observed seasonal changes in the SST is fairly good. However, the model-predicted MLD is shallower than observed in the spring and summer by about 10 m. This is due to the diffusion of heat out of the SML into the thermocline by the B_v wave mixing. This can be seen in the ISOD plot in Fig. 3, i.e., the predicted thermocline below the SML is now much weaker (more diffuse) than the observed thermocline.

Very noticeable in Fig. 3, relative to the previous simulations, is the large reduction of the model-predicted SST spikes. Notably, the very large SST spike in mid August that occurred in the simulations without the B_v wave mixing (e.g., Fig. 2) is completely gone. The observed SST does show a spike of about 1 °C at this time. Hence, this and a few other SST spikes are underpredicted.

However, the suppression of these SST spikes is due to mixing from the waves and swell that persist after the winds have died and, as noted above, there is considerable uncertainty regarding the wave dissipation used in SWAN and the prediction of wave propagation in a wave model run at a single location. Hence, the validity of the suppression of the SST spikes at Papa by the B_v wave mixing is uncertain.

Note that the Qiao et al. (2004) parameterization of the wave mixing takes no account of the density stratification. Hence, wave mixing within the seasonal thermocline will diffuse heat out of the SML into the thermocline and diffuse the thermocline; and during light-wind events, residual waves and swell will tend to suppress the formation of shallow mixed layers and SST spikes.

In summary, as used here with $\alpha = 1$, the Qiao et al. (2004) parameterization of wave mixing causes too much diffusion of heat out of the SML and too much diffusion within the thermocline below the SML in the summer. Additionally, residual waves and swell during light wind events
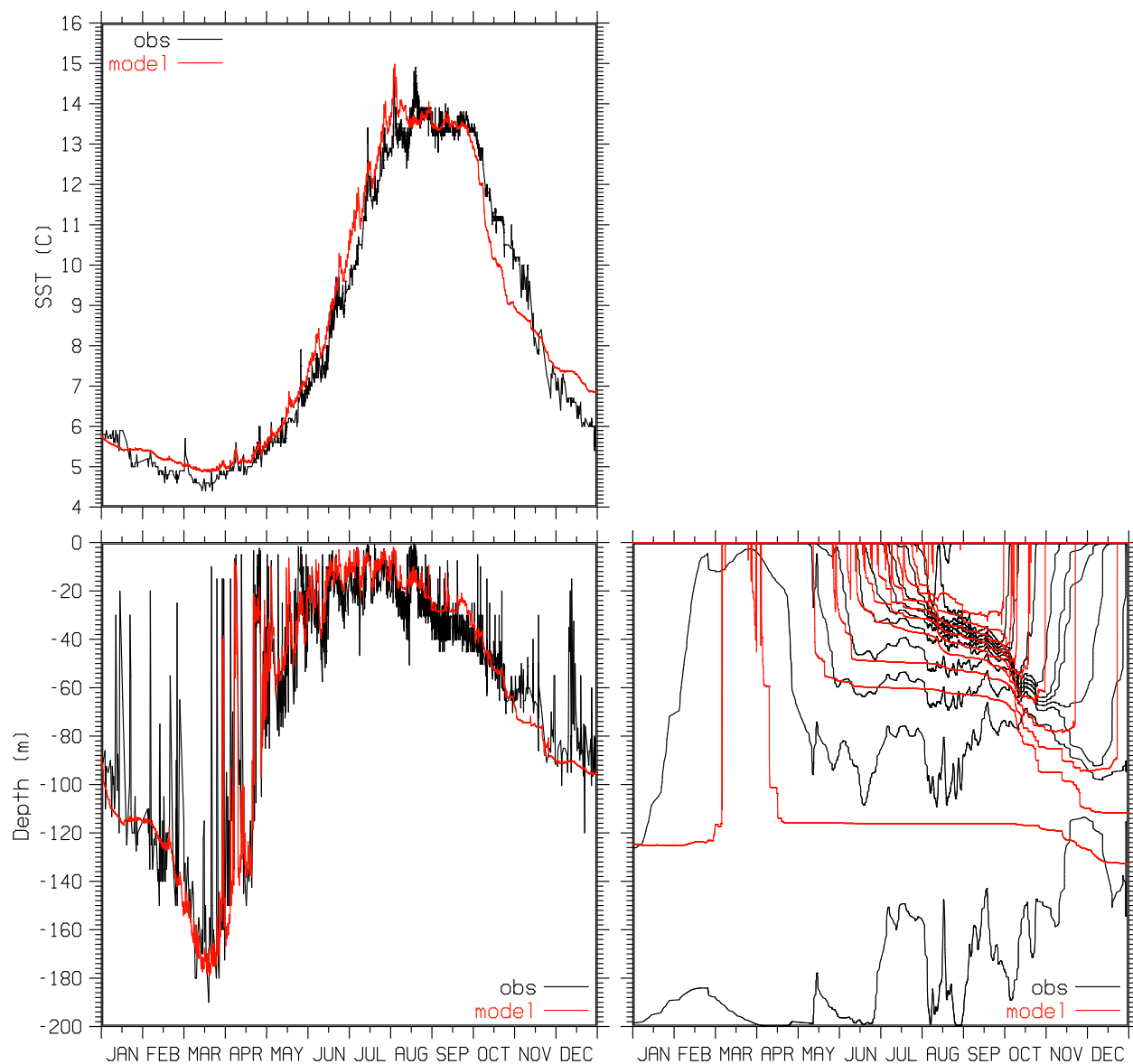
Fig. 3 — SST, MLD, and ISODs at OWS Papa for 1961: observed (black), simulated with MYL2 MLM with Qiao et al. (2004) wave mixing with $\alpha = 1$ (red)

can suppress the formation of shallow mixed layers and associated SST spikes, though there is significant uncertainty regarding this aspect of the wave prediction by SWAN at Papa.

Since several of the papers discussing direct wave mixing describe a fairly large uncertainty regarding the level of mixing generated by the waves (Qiao et al. 2004; Babanin 2006), it was decided to try a lower level of wave mixing with the scaling factor α in Eq. (1) reduced from 1 to 0.1.

Figure 4 shows results from a simulation of the SML at Papa for 1961 with the MYL2 MLM (without the enhanced mixing of Large et al. 1994) and with the wave mixing from Qiao et al. (2004) scaled with $\alpha = 0.1$. With the wave mixing reduced by 90%, there is not enough mixing and the SST is about 2 °C too high and the MLD is about 10 to 15 m too shallow in the spring and summer.

To increase the MLDs, the mixing enhancement of Large et al. (1994) was added back to the MYL2 MLM, and the results for the wave mixing with α reduced to 0.1 are shown in Fig. 5. With the combination of decreased mixing from the waves and increased mixing from the Large et al. (1994) mixing enhancement, the predicted SST is quite good. The SST spikes are reduced relative to the simulations without the wave mixing, but are larger than with the full wave mixing. The predicted MLD is also quite good, being perhaps 5 to 10 m too shallow at various times in spring and summer. The predicted ISODs, like the MLDs, are about 5 m too shallow in the summer. The predicted ISODs are much less diffused than with the full Qiao et al. (2004) wave mixing.

In summary, with reduced wave mixing with $\alpha = 0.1$, there is less diffusion of the thermocline below the SML at Papa in the summer and the agreement of the predicted ISODs with the observed ISODs is better than with the full wave mixing with $\alpha = 1$.

3. SIMULATION OF MIXED LAYER AT NOAA BUOY 46005

3.1 Data for Buoy 46005

For the purpose of evaluating the performance of a wave-mixing parameterization in light-wind conditions, performing simulations at OWS Papa involves considerable uncertainty in predicting the wave conditions during periods of light winds, since running a wave model at a single location makes it difficult to account for swell that propagates to that location from other areas. There is also some uncertainty as to the accuracy of the SSTs obtained at Papa from the MBTs.

This led us to consider performing mixed-layer simulations at the locations of some of the NOAA buoys, since the buoys can provide surface marine observations for computing the surface wind and heat-flux forcing for a local mixed-layer simulation and can also provide spectral wave observations that can be used to compute wave mixing, i.e., the B_v wave-mixing profiles of Qiao et al. (2004) can be computed directly from wave observations (which include swell) rather than from having to run a wave model. The buoys also measure the seawater temperature fairly close to the surface, so their seawater temperature measurements should provide a fairly good estimate of the local SST.

Unfortunately, the NOAA buoys do not generally have subsurface observations. The lack of subsurface temperature observations does not allow evaluation of the simulated subsurface thermal
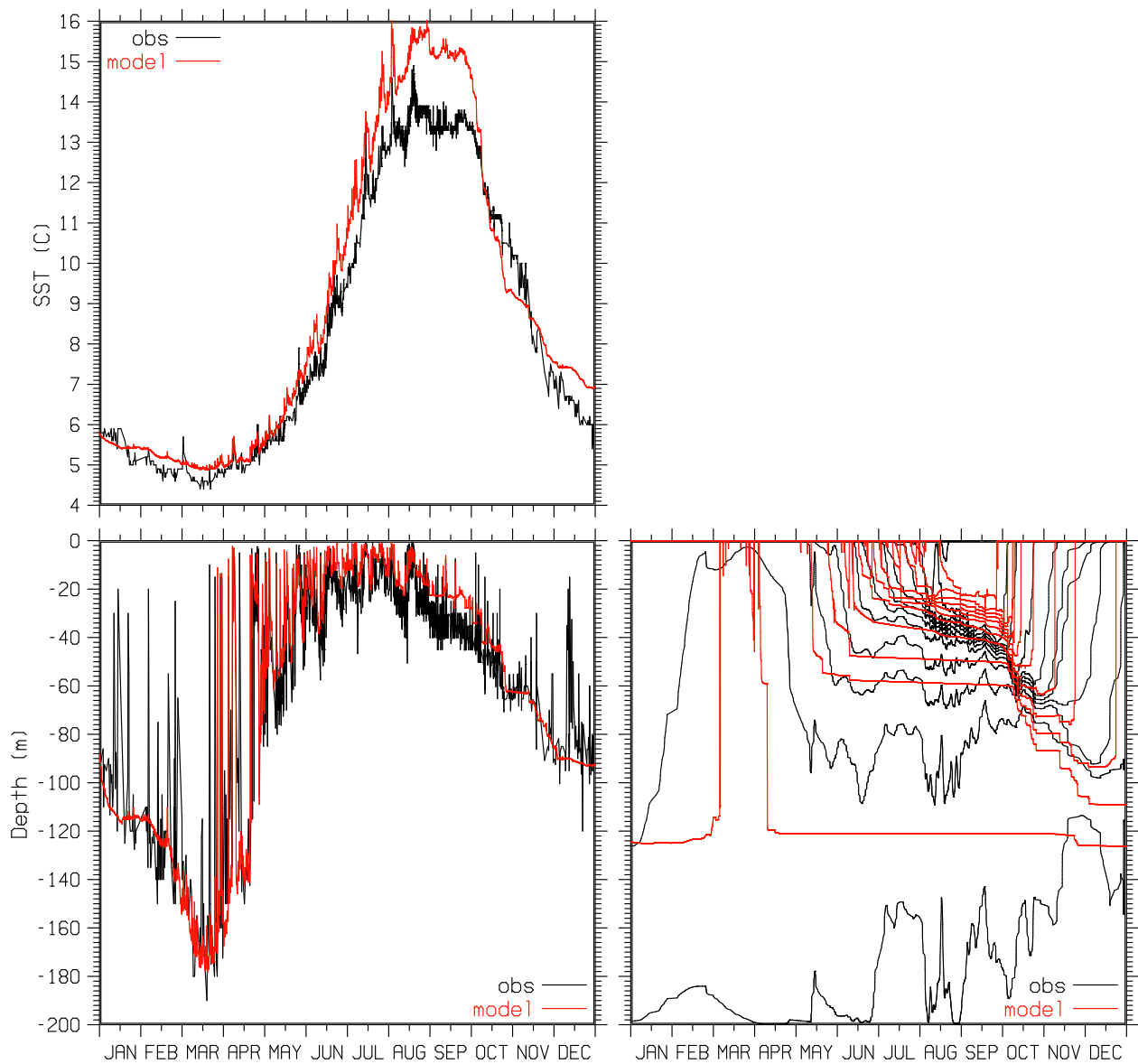
Fig. 4 — SST, MLD, and ISODs at OWS Papa for 1961: observed (black), simulated with MYL2 MLM
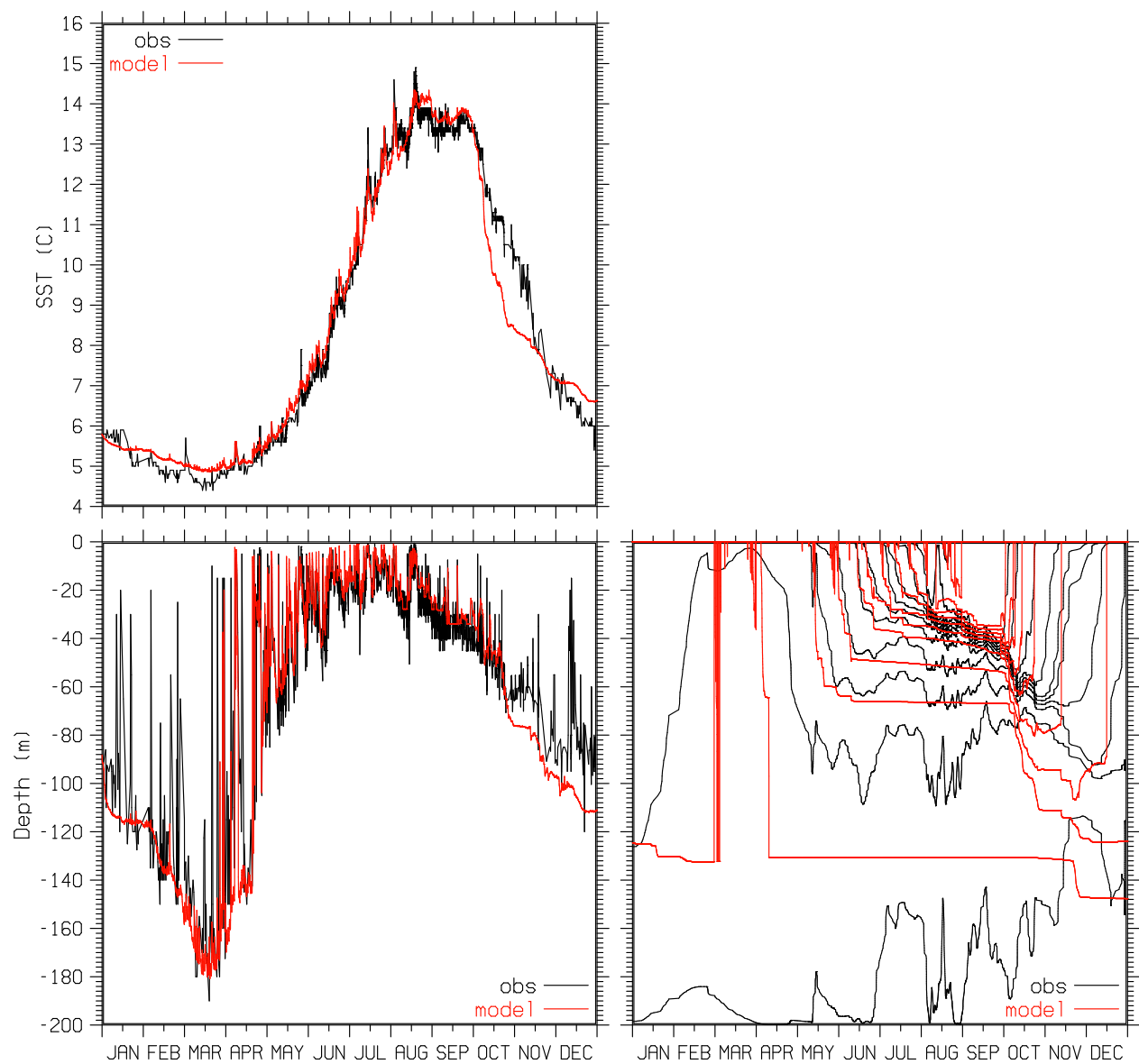with reduced Qiao et al. (2004) wave mixing with $\alpha = 0.1$ (red)

Fig. 5 — SST, MLD, and ISODs at OWS Papa for 1961: observed (black), simulated with MYL2 MLM with reduced Qiao et al. (2004) wave mixing with $\alpha = 0.1$ and with Large et al. (1994) mixing enhancement (red)

structure and possible biases in the surface heat fluxes used for the simulation. However, the buoy SST observations do allow looking at SST spikes that occur during periods of light winds due to the formation of shallow mixed layers, and these simulated SST spikes are not very sensitive to small-to-moderate biases in the surface heat fluxes that are used. Both real-time and archived buoy observations can easily be downloaded from the NOAA NDBC web site at http://www.ndbc.noaa.gov.

The first buoy that was looked at was NOAA Buoy 46005, which is located in the northeast Pacific at 131.001 °W, 46.100 °N, which is about 1100 km ESE of the location of OWS Papa. We had hoped to find a buoy closer to OWS Papa at 145 °W, 50 °N, but a suitable buoy near that location was not found.

NOAA Buoy 46005 is a 3-m discus buoy. The water depth at this location is 2981 m. Meteorological and spectral wave data from this buoy are available since 1976. The data from this buoy used for this report are for the year 2000, since this year has a fairly complete set of both meteorological and wave observations.

The observations at Buoy 46005 include wind speed and direction (measured by an anemometer at 5-m height), air temperature (measured at a height of 4 m), surface air pressure, and SST (measured at a depth of 0.6 m below the sea surface). Two additional observations needed to compute the surface heat fluxes, solar insolation (or cloud cover) and humidity, were not available. Hence, for cloud cover and humidity, monthly climatology from OWS Papa, computed from the surface marine observations at Papa between 1960 and 1970, was used.

The use of climatological humidity should provide a reasonably good estimate at a location in the open sea. However, the use of climatological cloud cover will likely underestimate the solar heating that occurs during some of the light-wind periods, since periods of light winds are sometimes associated with the interior of high-pressure systems, which are associated with clear skies. A couple of factors that help mitigate the problems of using climatological cloud cover are (1) this area of the Pacific is notoriously cloudy (the mean cloud cover at Papa is about 83%), and (2) SST spikes are much more dependent on the occurrence of light winds than clear skies.

Note that, since the focus of the mixed-layer simulations conducted with the buoy data are the SST spikes that occur during periods of light winds, possible biases in the surface heat flux are not as critical as they would be if the focus were on simulating the seasonal evolution of the SST.

Figure 6 shows SST, wind speed, and significant wave height at Buoy 46005 for the year 2000. For this year, there are only a couple of significant SST spikes, one near the beginning of June and another near the end of July. Both of these spikes occur during periods of light winds. A notable feature of the significant wave height is that it rarely drops below a value of about 1 m, even during periods of light winds. This is primarily due to swell that has propagated from other areas.

Atmospheric forcing for the model simulations conducted at Buoy 46005 was computed using the buoy observations discussed above, standard bulk formulas for the wind stress and the latent and sensible heat fluxes (Wyrtki 1965), and the drag coefficient formulas from Large and Pond (1981). Adjustment to account for the height above sea level of the marine observations was computed using the Businger-Dyer boundary-layer flux profiles (Liu et al. 1979). Solar radiation was computed using the Fritz formula for clear-sky insolation (List 1958) with the Tabata (1964) cloud-cover correction, and net longwave radiation was computed using the formula of Berliand (1960). A 6% albedo was
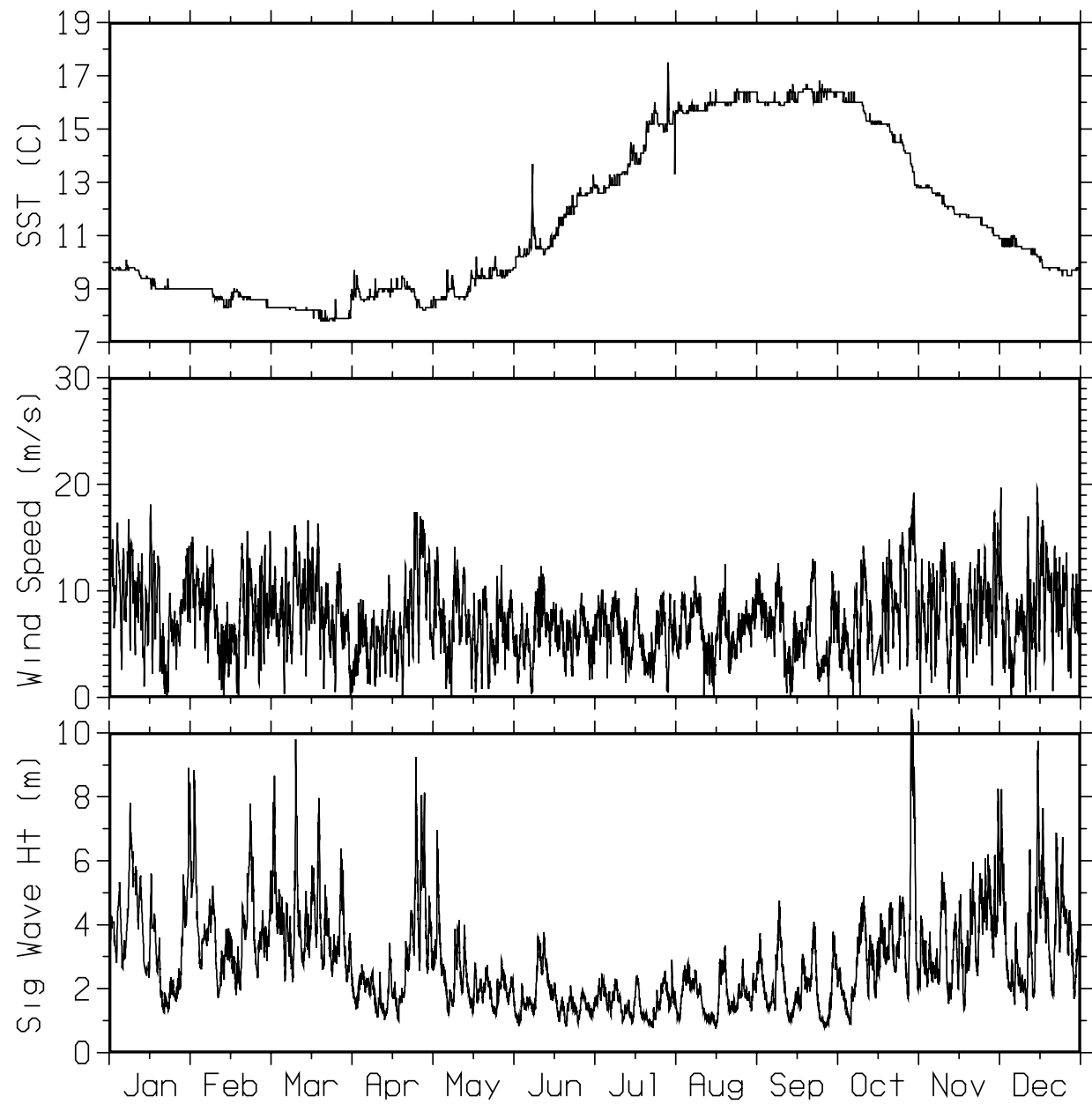
Fig. 6 — SST, wind speed, and significant wave height at Buoy 46005 for the year 2000

assumed for the solar radiation ($F_r = 0.94$) and the the net longwave radiation and the latent and sensible heat fluxes were used as computed without adjustment ($F_e = 1.0$).

Without subsurface temperature observations, it is difficult to determine if the heat input by the surface heat fluxes is a good match for the actual change in the upper-ocean heat content. The solar extinction and ambient diffusivity were as used for the simulations at Station Papa (Jerlov Type II and 0.02 cm^2/s, respectively). The initial T and S profiles for the simulation were taken from the Levitus (1982) climatology at the location of the buoy for the beginning of January.

3.2 Results for Buoy 46005

Figure 7 shows the observed and simulated SST for a simulation at Buoy 46005 for the year 2000 conducted with the MYL2 MLM with the Large et al. (1994) mixing enhancement, but without the B_v wave mixing of Qiao et al. (2004). The simulated temperatures shown in the SST plot were uniformly reduced by 1 °C to better match the observed temperatures (note that this is equivalent to decreasing the initial T profile by a uniform 1 °C).

The seasonal variability of the simulated SST in Fig. 7 agrees very well with the variability of the observed SST in spring and fall, but is about 1 °C too high in mid summer. The simulation shows the same two large SST spikes as the observed SST at exactly the same times. The simulated spike in early June is about 1 °C smaller than observed, i.e., 1.5 °C vs 2.5 °C observed. However, the simulated spike in late July is similar in magnitude to the observed spike, both being close to 2 °C.

Figure 8 shows the observed and simulated SST for a simulation at Buoy 46005 for the year 2000 conducted with the MYL2 MLM with the full ($\alpha = 1$) B_v wave mixing of Qiao et al. (2004), but without the Large et al. (1994) mixing enhancement. As in Fig. 7, the simulated temperatures shown in the plot were uniformly reduced by 1 °C.

The seasonal variability of the simulated SST in Fig. 8 agrees well with the observed seasonal SST variability in the spring, but is 1 to 2 °C too high for the period August through November. The SST spikes that are observed in spring and summer are all suppressed, including the two largest SST spikes observed in early June and late July. It is apparent that the B_v wave mixing computed from the swell observed at Buoy 46005 during periods of light winds in Fig. 6 is sufficient to prevent very shallow mixed layers and large SST spikes from occurring in the simulation.

Figure 9 shows the observed and simulated SST for a simulation at Buoy 46005 for the year 2000 conducted with the MYL2 MLM without the Large et al. (1994) mixing enhancement with the B_v wave mixing of Qiao et al. (2004) reduced by 90% ($\alpha = 0.1$). With the reduced values of the B_v wave-mixing profiles and without the Large et al. (1994) mixing enhancement, the simulated SST in spring and summer becomes warmer than the observed SST. The SST spikes are larger than with the full B_v wave mixing in Fig. 8, but most of the SST spikes are still smaller than those observed, and the large SST spikes observed in early June and late July are much smaller than observed.
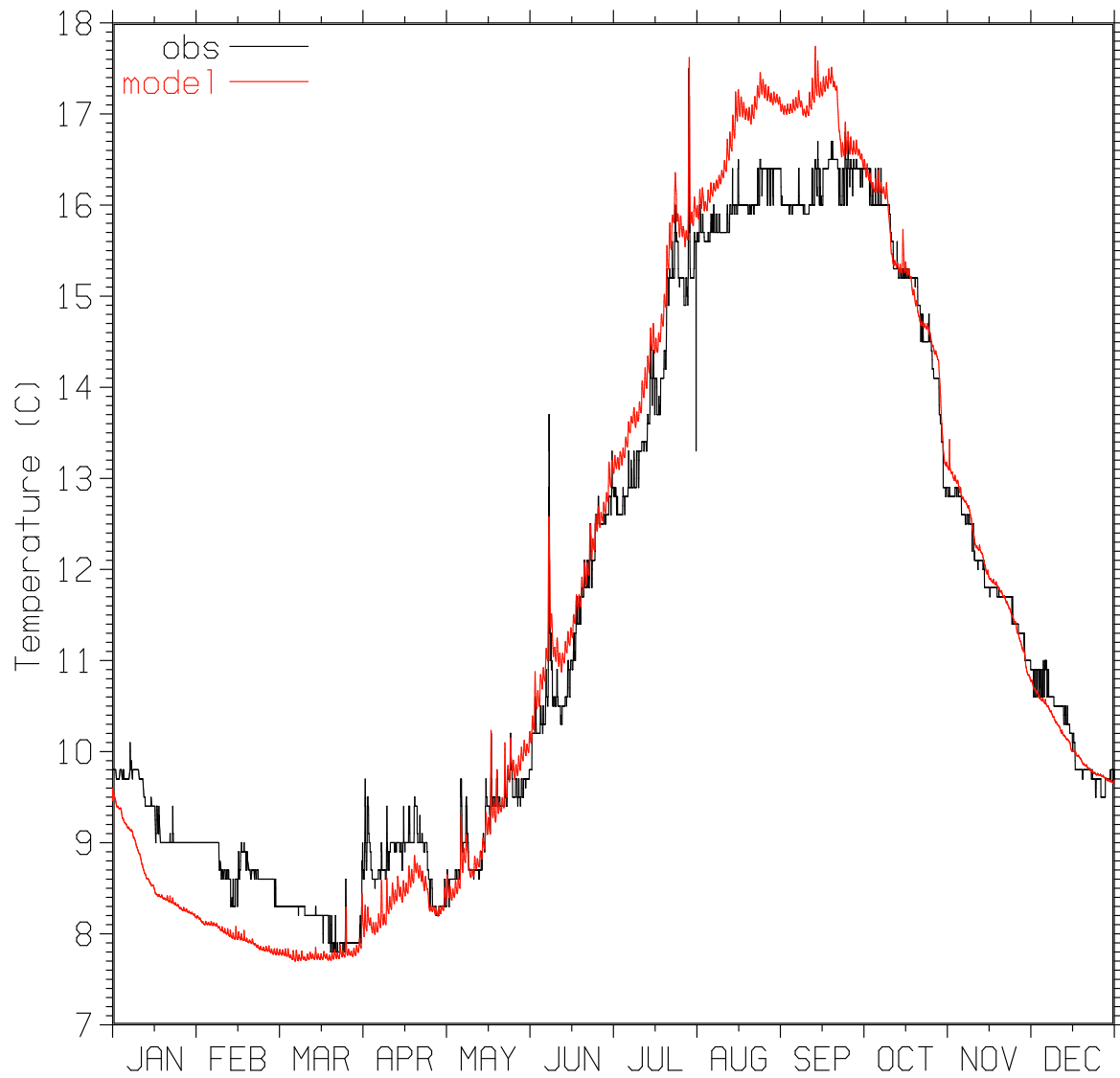
Fig. 7 — SST at Buoy 46005 for the year 2000: observed (black), simulated with MYL2 MLM with Large
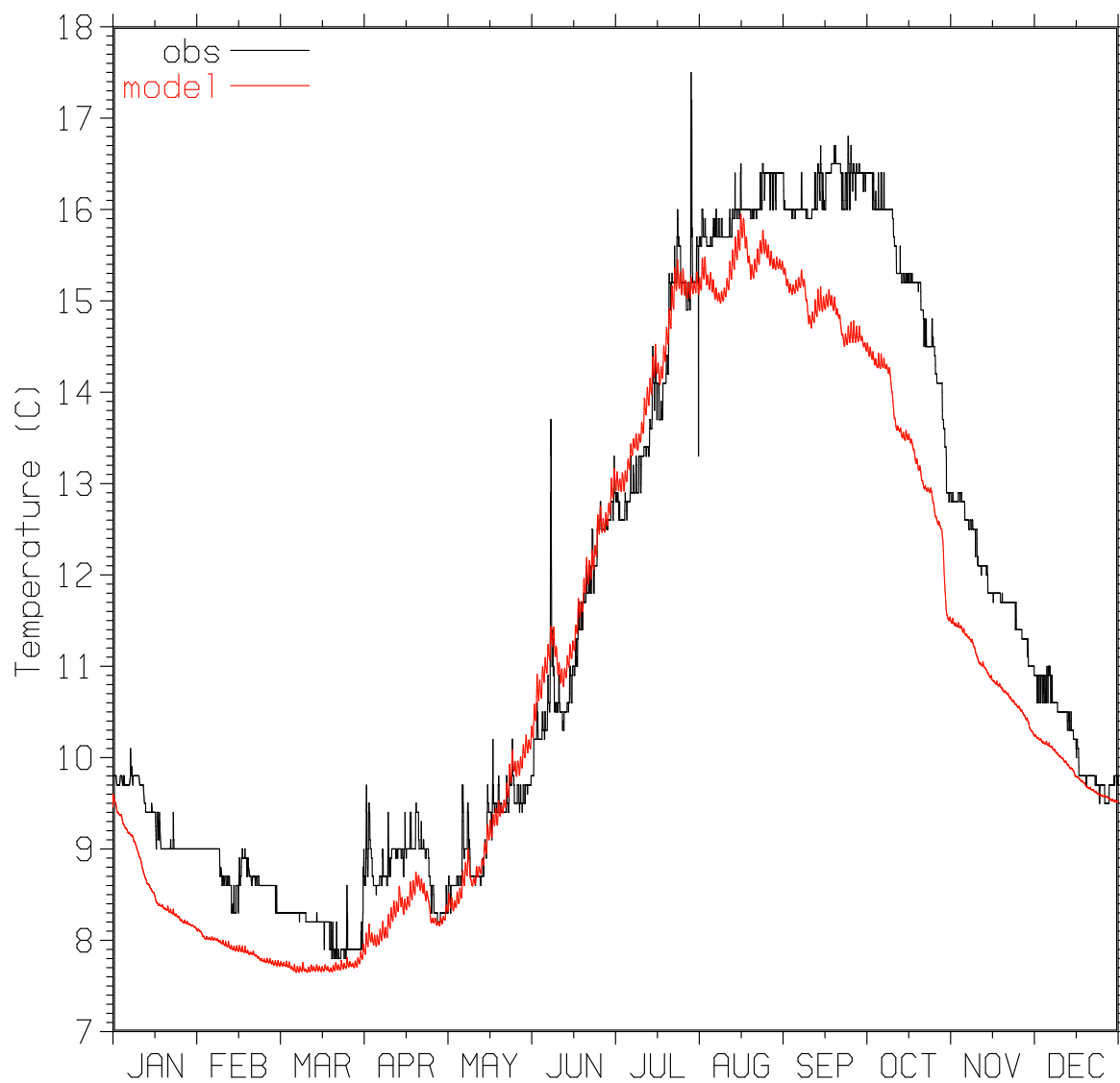et al. (1994) mixing enhancement (red)

Fig. 8 — SST at Buoy 46005 for the year 2000: observed (black), simulated with MYL2 MLM with Qiao et al. (2004) wave mixing with $\alpha = 1$ (red)
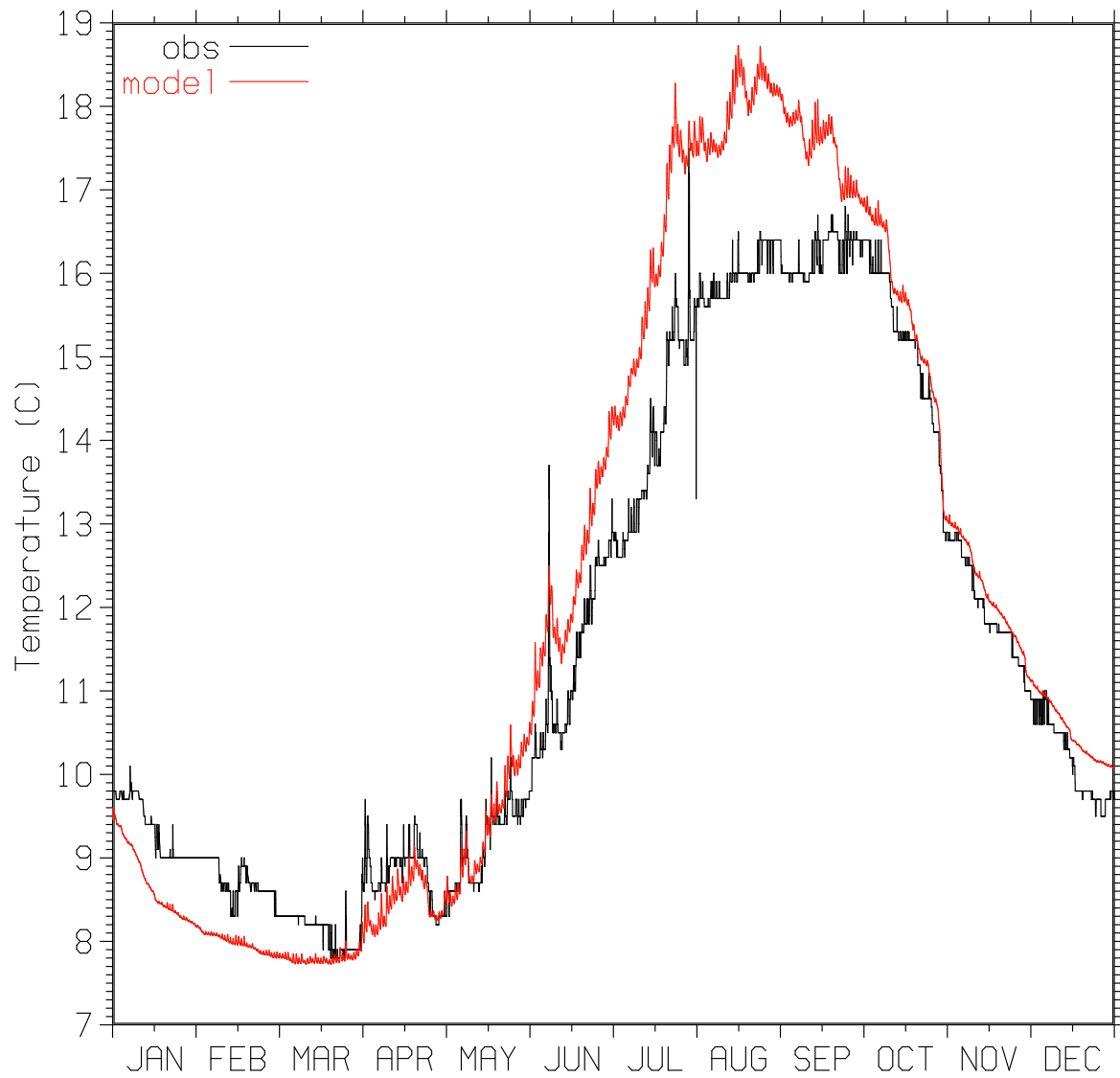
Fig. 9 — SST at Buoy 46005 for the year 2000: observed (black), simulated with MYL2 MLM with reduced Qiao et al. (2004) wave mixing with $\alpha = 0.1$ (red)

4. SIMULATION OF MIXED LAYER AT NOAA BUOY 46047

4.1 Data for Buoy 46047

The observations from Buoy 46005 show only two large SST spikes during the year 2000. One reason there are not more SST spikes observed in Fig. 6 is that the winds tend to be relatively strong at this latitude. We considered that the chance of seeing more SST spikes would increase at a buoy further south where the winds are generally lighter; hence, we looked at data from NOAA Buoy 46047 located in the northeast Pacific at 119.533 °W, 32.433 °N.

Buoy 46047 is also a 3-m discus buoy. The water depth at the location of Buoy 46047 is 1394 m. Meteorological and spectral wave data from this buoy are available since 1991. We used data from the year 2004, since this year has a fairly complete set of meteorological and wave observations for Buoy 46047.

The observations available from Buoy 46047 are similar to those available from Buoy 46005, and as for 46005, cloud cover and humidity data are not available. Monthly climatology for humidity was taken from OWS November at 140 °W, 30 °N, which was computed from the surface marine observations taken at November between 1960 and 1972. Cloud cover was taken from the monthly averaged data available from the International Satellite Cloud Climatology Project (ISCCP) (Schiffer and Rossow 1983) for 2004. The ISCCP cloud-cover data consist of monthly averaged values of 3-h cloud cover for the period 1983 to 2008, i.e., the data represent the mean, diurnal cycle of cloud cover for each month from 1983 to 2008. The mean diurnal cycle of cloud cover is useful for computing solar radiation in case there is a significant mean diurnal variation of the cloud cover.

Figure 10 shows SST, wind speed, and significant wave height at Buoy 46047 for the year 2004. For this year, there are a number of significant SST spikes, many more than were observed at Buoy 46005 for the year 2000. As observed at Buoy 46005, the significant wave height rarely drops below a value of about 1 m, even during periods of very light winds.

Atmospheric forcing for the model simulations conducted at Buoy 46047 was computed using the buoy observations, the ISCCP monthly averaged diurnal cycles of cloud cover for 2004, the monthly climatological humidity from OWS November, and the air-sea flux formulas used for Buoy 46005 in Section 3.1, except that the Reed (1977) cloud-cover correction was used to compute the solar radiation. A 6% albedo was assumed for the solar radiation ($F_r = 0.94$), the net longwave radiation was used as computed, and the latent and sensible heat fluxes were reduced by 5% ($F_e = 0.95$) to provide a better match between the observed and simulated seasonal SST cycle. The mean computed heat fluxes are 178.0 W/m^2 for solar and -171.4 W/m^2 for the surface heat flux, which give 6.6 W/m^2 for the total heat flux. The solar extinction was taken to be Jerlov Type II and ambient diffusion was set to 0.02 cm^2/s. The initial T and S profiles for the simulation were taken from the Levitus (1982) climatology at the location of the buoy for the beginning of January.

4.2 Results for Buoy 46047

Figure 11 shows the observed and simulated SST for a simulation at Buoy 46047 for the year 2004 conducted with the MYL2 MLM with the Large et al. (1994) mixing enhancement, but without the B_v wave mixing of Qiao et al. (2004).
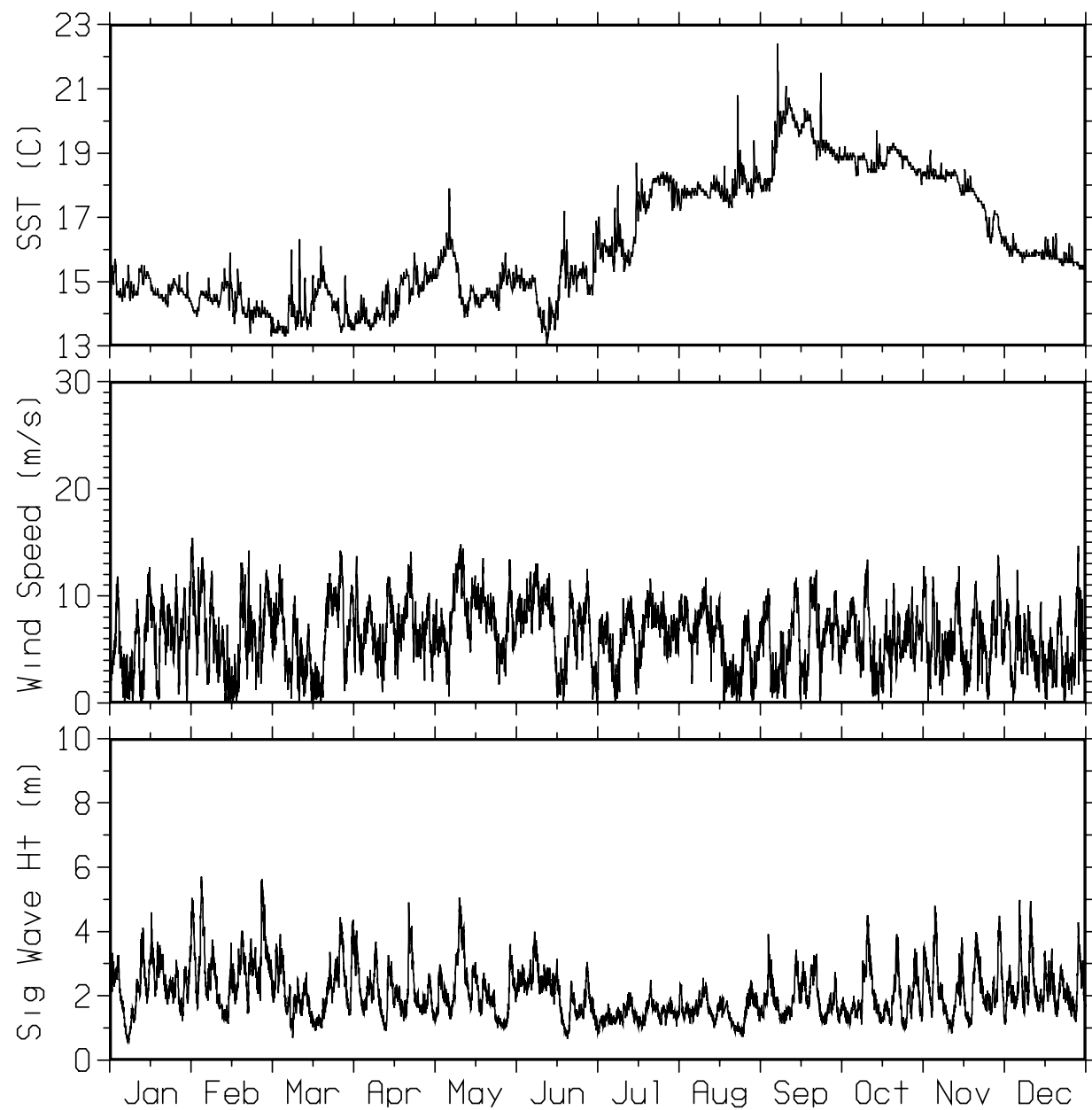
Fig. 10 — SST, wind speed, and significant wave height at Buoy 46047 for the year 2004
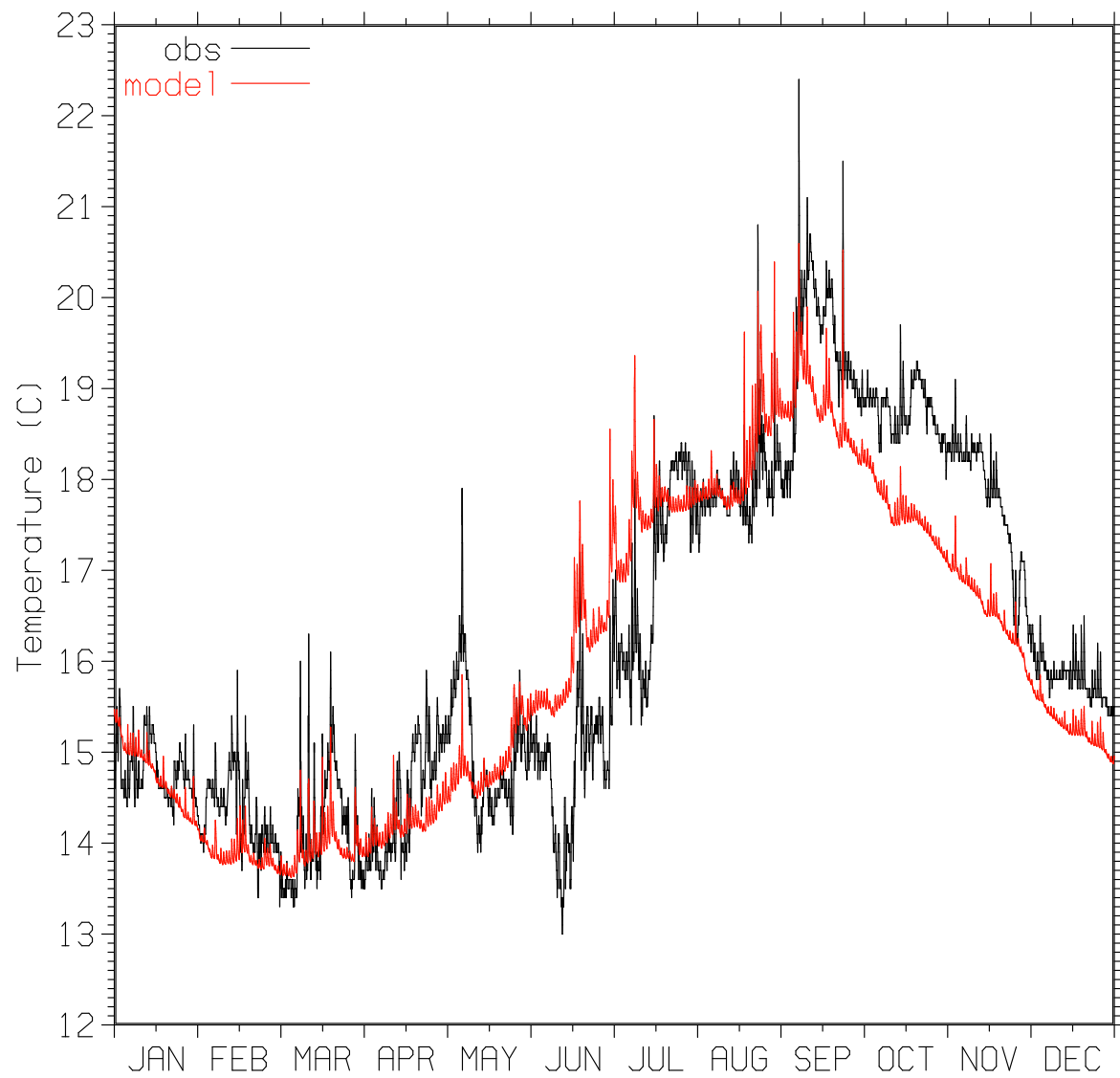
Fig. 11 — SST at Buoy 46047 for the year 2004: observed (black), simulated with MYL2 MLM with Large et al. (1994) mixing enhancement (red)

The seasonal variability of the simulated SST in Fig. 11 agrees fairly well with the observed seasonal SST variability, though the simulated SST is about 1 °C below the observed SST for the period September through December and there is a lot of variability in the observed SST on time scales of a few days to a couple of months that is not reproduced by the model simulation, which we guess may be due to advection.

The simulation shows SST spikes that are comparable to the observed spikes, though sometimes they are larger and sometimes they are smaller. This discrepancy may be due in part to the use of monthly averaged cloud cover and humidity in the simulation. In winter, the observations consistently show larger SST spikes than the simulation. This may be due to shallow mixed layers formed by or enhanced by advection, which the simulation does not account for.

Figure 12 shows the observed and simulated SST for a simulation at Buoy 46047 for the year 2004 conducted with the MYL2 MLM without the Large et al. (1994) mixing enhancement, but with the full ($\alpha = 1$) B_v wave mixing of Qiao et al. (2004).

The seasonal variability of the simulated SST in Fig. 12 agrees fairly well with that observed in the spring and summer but, as for the simulation without the wave mixing, is lower than observed in the fall. The SST spikes are strongly suppressed by the B_v wave mixing. As at Buoy 46005, it is apparent that the B_v wave mixing computed from the swell observed at Buoy 46047 during periods of light winds (Fig. 10) is sufficient to prevent very shallow mixed layers and SST spikes from occurring.

Figure 13 shows the observed and simulated SST for a simulation at Buoy 46047 for the year 2004 conducted with the MYL2 MLM without the Large et al. (1994) mixing enhancement and with the B_v wave mixing of Qiao et al. (2004) reduced by 90% ($\alpha = 0.1$). With the reduced wave mixing, the seasonal variability of the simulated SST is higher than observed in the spring and summer, but is fairly good for the period September through December. The SST spikes are larger than with the full B_v wave mixing in Fig. 12, but most of the SST spikes are still smaller than those observed and smaller than those simulated without the wave mixing in Fig. 11.

5. SIMULATION OF MIXED LAYER AT NOAA BUOY 41049

5.1 Data for Buoy 41049

NOAA Buoy 41049, which is a 6-m NOMAD buoy, is located in the Sargasso Sea in the northwest Atlantic at 63.000 °W, 27.500 °N. This area has a couple of advantages for the present purposes of simulating the SML, since (a) the winds in this area are relatively light and there should be a fair number of SST spikes due to the formation of shallow mixed layers, and (b) the effect of advection in this central gyre region should be small, at least on seasonal and longer time scales.

The water depth at the location of Buoy 41049 is 4885 m. Meteorological and spectral wave data from this buoy are available only since May 2009. There is a very abrupt drop in the observed SST at Buoy 41049 in August 2009 of 2 °C, which is unusual for this time of year and is probably due to Hurricane Bill, which passed just to the southwest of Buoy 41049 on August 21. We thought it would be interesting to perform SML simulations at this buoy during this time to see if the simulations would reproduce this feature as well as the SST spikes.
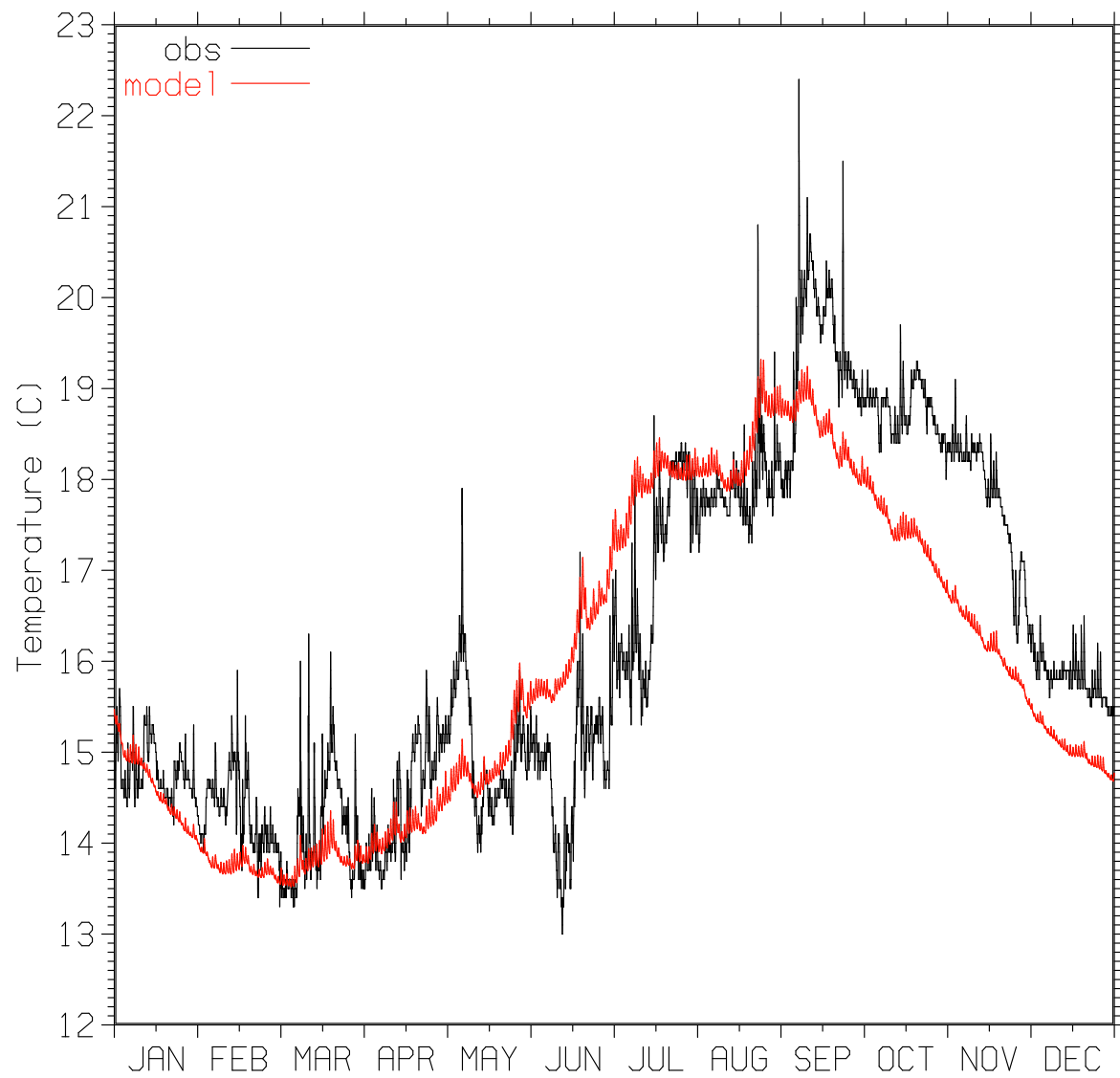
Fig. 12 — SST at Buoy 46047 for the year 2004: observed (black), simulated with MYL2 MLM with Qiao et al. (2004) wave mixing with $\alpha = 1$ (red)
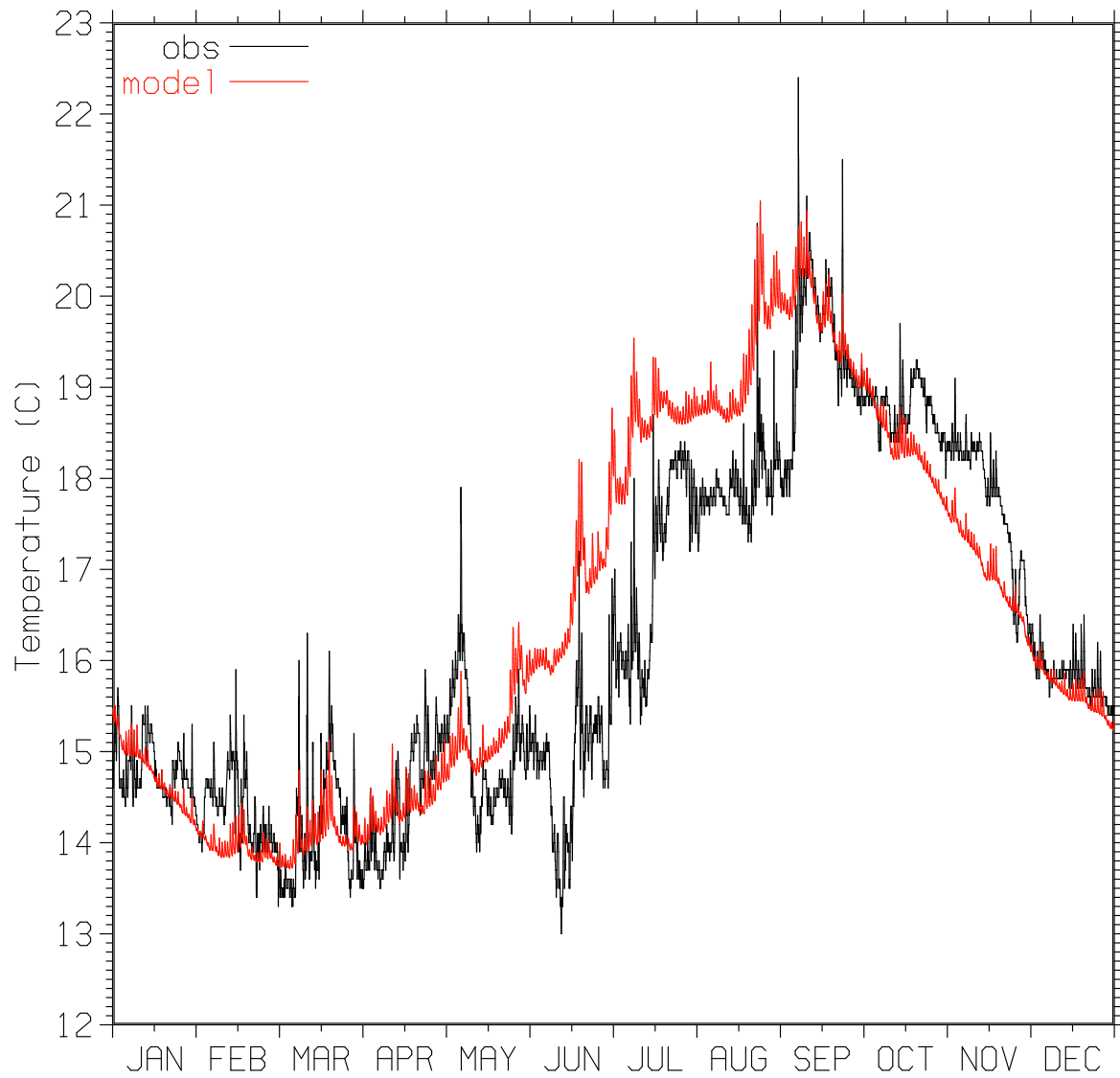
Fig. 13 — SST at Buoy 46047 for the year 2004: observed (black), simulated with MYL2 MLM with reduced Qiao et al. (2004) wave mixing with $\alpha = 0.1$ (red)

The observations available from Buoy 41049 are similar to those available from Buoys 46005 and 46047, i.e., wind speed and direction are measured at 5-m height, the air temperature is measured at 4-m height, and the air pressure is measured at sea level. The water temperature is measured at a depth of 1 m. Cloud cover and humidity data are not available. Cloud cover data from the ISCCP, which were used for Buoy 46047, are currently not available for 2009. Based on the ISCCP cloud data for this location for earlier years, a constant cloud-cover fraction of 0.5 was used. Monthly climatology for humidity was taken from OWS November at 140 °W, 30 °N, which is at a similar latitude.

Figure 14 shows SST, wind speed, and significant wave height at Buoy 41049 for the period May through December 2009. There are a number of spikes in the observed SST of 1 °C or more, and there is a very sharp SST drop of about 2 °C in August, which is coincident with a short, high-wind event with a maximum wind speed of 20 m/s and a large spike in the significant wave height.

Atmospheric forcing for the simulations conducted at Buoy 41049 were computed using the buoy observations, a constant cloud fraction of 0.5, the monthly climatological humidity from Station November, and the the air-sea flux formulas used for Buoy 46047 in Section 4.1. A 6% albedo was assumed for the solar radiation ($F_r = 0.94$), the net longwave radiation was used as computed, and the latent and sensible heat fluxes were reduced by 5% ($F_e = 0.95$) to provide a better match between the observed and simulated seasonal SST cycles. The mean computed heat fluxes for May through December are 217.6 W/m^2 for solar radiation and -218.1 W/m^2 for the surface heat fluxes, which give -0.5 W/m^2 for the total mean heat flux for May through December 2009. The solar extinction was taken to be Jerlov Type IA (Jerlov 1976) and the ambient diffusivity was 0.02 cm^2/s. The initial T and S profiles for the simulation were taken from the Levitus (1982) climatology at the location of the buoy for the middle of May.

5.2 Results for Buoy 41049

Figure 15 shows the observed and simulated SST for a simulation at Buoy 41049 for May through December 2009 conducted with the MYL2 MLM with the Large et al. (1994) mixing enhancement, but without the B_v wave mixing of Qiao et al. (2004).

The seasonal variability of the simulated SST in Fig. 15 agrees fairly well with that observed, though the simulated SST is offset about 1 to 2 °C below the observed SST. This offset could have been reduced by adjusting the initial temperature profile, but it was decided to retain the offset to make it easier to compare the details of the simulated and observed SST in the plot. There is some variability in the observed SST on time scales of a few days to a month that is not reproduced by the model simulation, which may be due to advection. The sharp drop in SST in August is reproduced fairly well, but the simulated SST drop is about 0.5 °C less than the observed drop.

The simulation shows SST spikes that are generally comparable to the observed spikes in spring and summer. In fall and winter, the observations consistently show larger SST spikes than the simulation, which may be due to shallow mixed layers formed by or enhanced by advection, which the simulation does not account for.
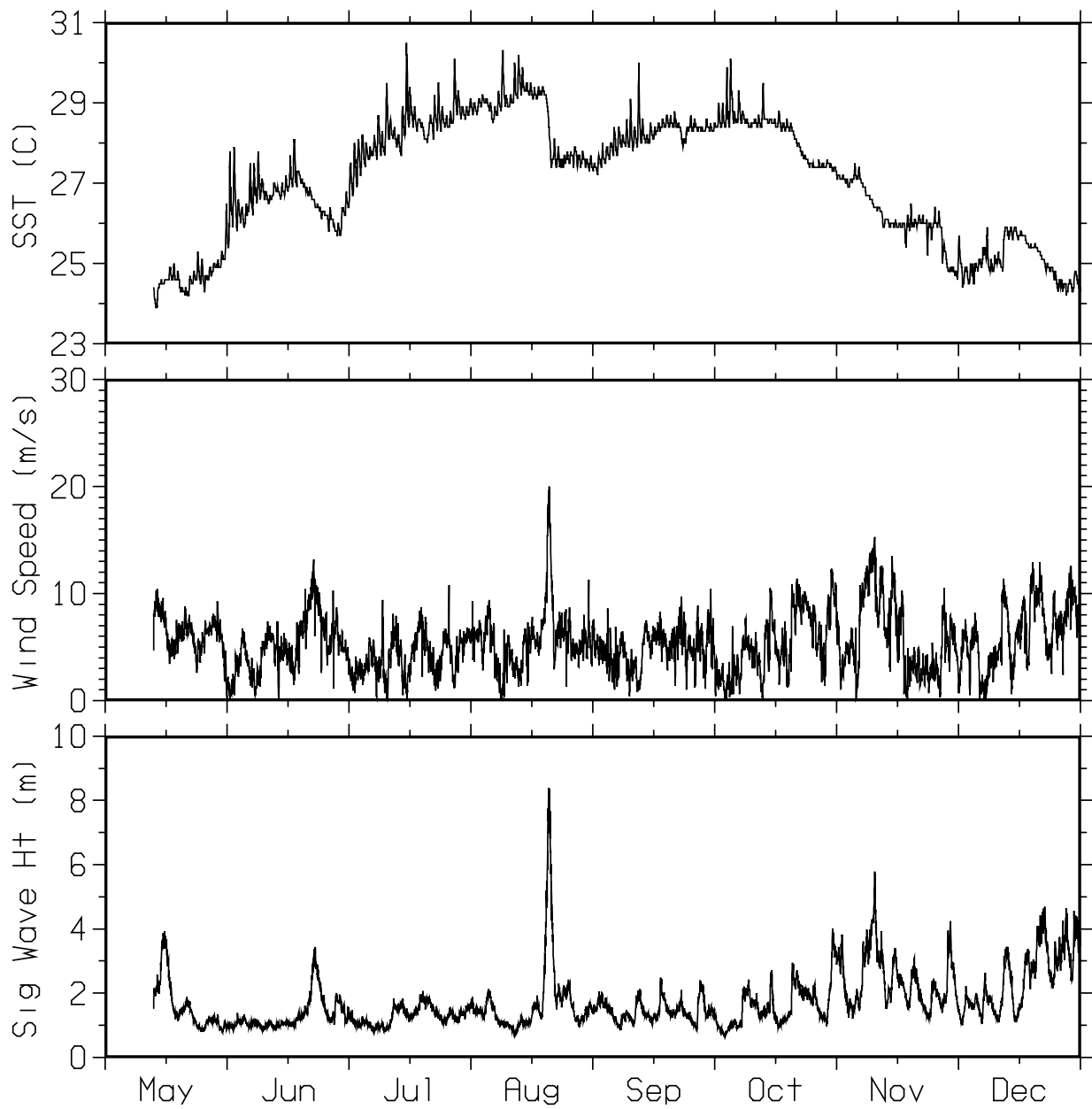
Fig. 14 — SST, wind speed, and significant wave height at Buoy 41049 for May through December 2009
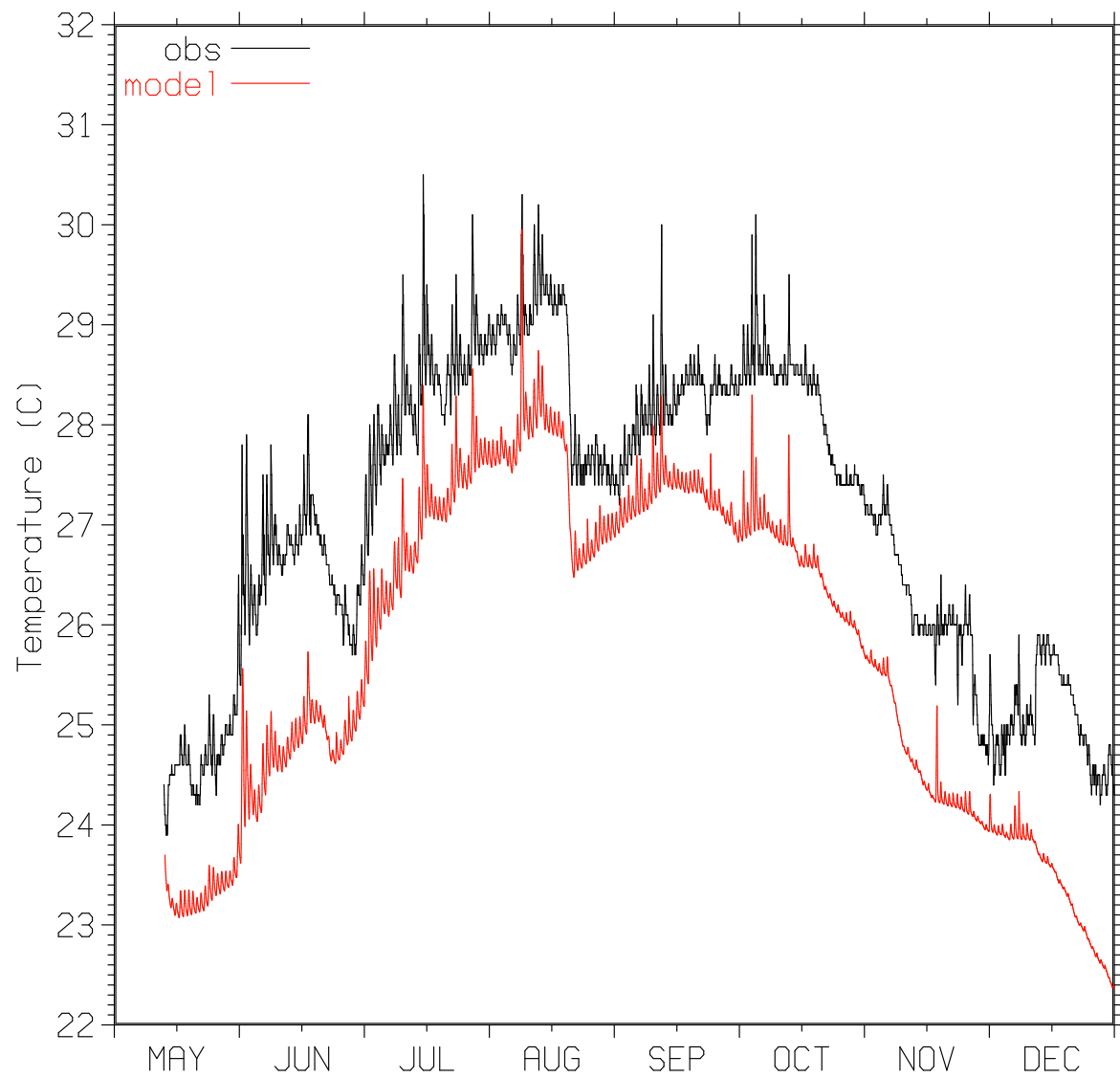
Fig. 15 — SST at Buoy 41049 for May through December 2009: observed (black), simulated with MYL2 MLM with Large et al. (1994) mixing enhancement (red)
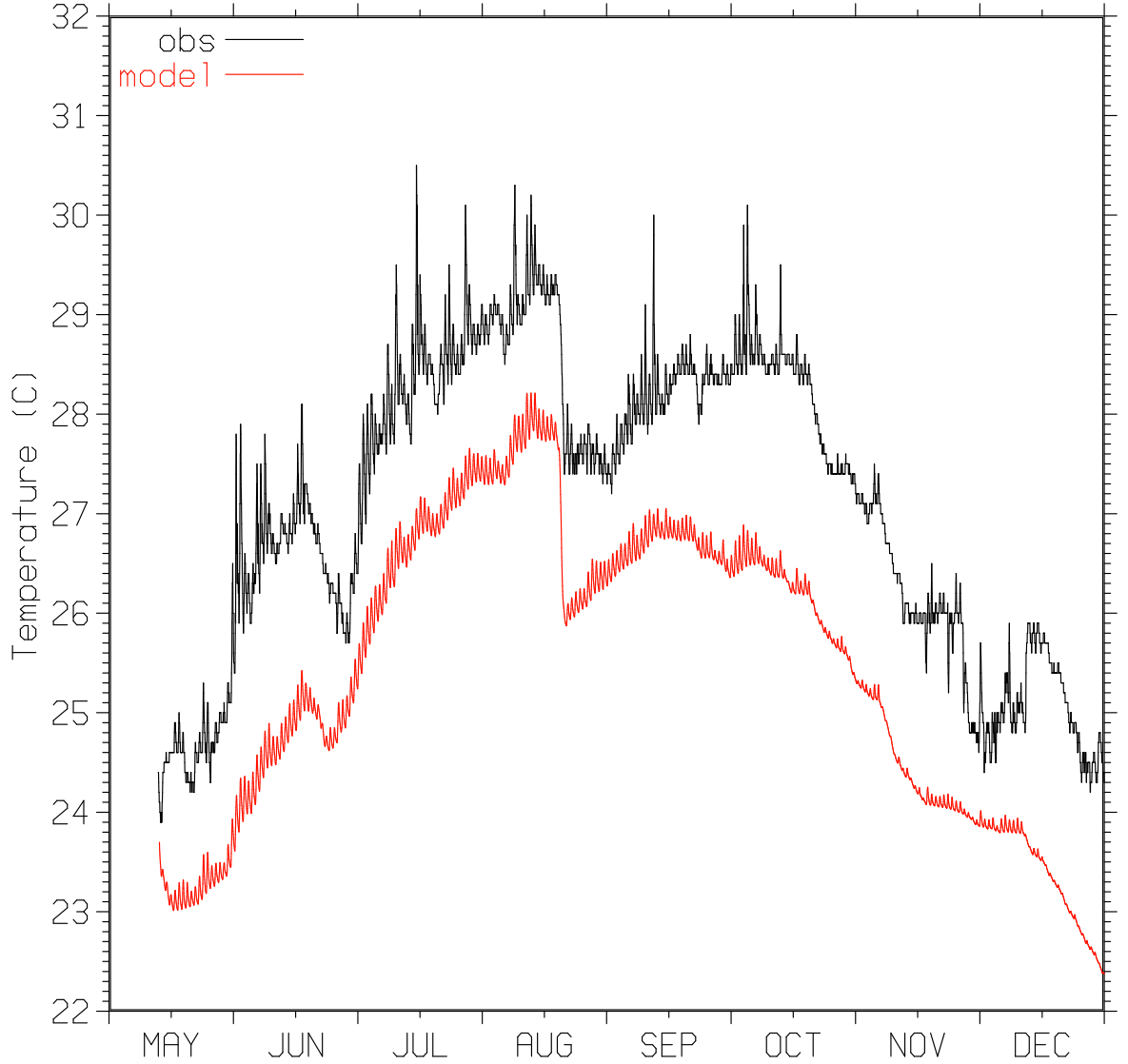
Fig. 16 — SST at Buoy 41049 for May through December 2009: observed (black), simulated with MYL2 MLM with Qiao et al. (2004) wave mixing with $\alpha = 1$ (red)

Figure 16 shows the observed and simulated SST for a simulation at Buoy 41049 for May through December 2009 conducted with the MYL2 MLM without the Large et al. (1994) mixing enhancement, but with the full ($\alpha = 1$) B_v wave mixing of Qiao et al. (2004).

The seasonal variability of the simulated SST in Fig. 16 agrees fairly well with the seasonal variability of the observed SST. The SST spikes are strongly suppressed by the B_v wave mixing. As at the other buoys, it is apparent that the B_v wave mixing computed from the swell observed at Buoy 41049 during periods of light winds (Fig. 14) is sufficient to prevent very shallow mixed layers and SST spikes from occurring. However, the magnitude of the simulated SST drop in August of about 2 °C agrees well with the magnitude of the observed drop. The large waves observed at this time (Fig. 14) appear to contribute towards increasing the mixing in the simulation relative to the simulation without the Qiao et al. (2004) wave-mixing parameterization.
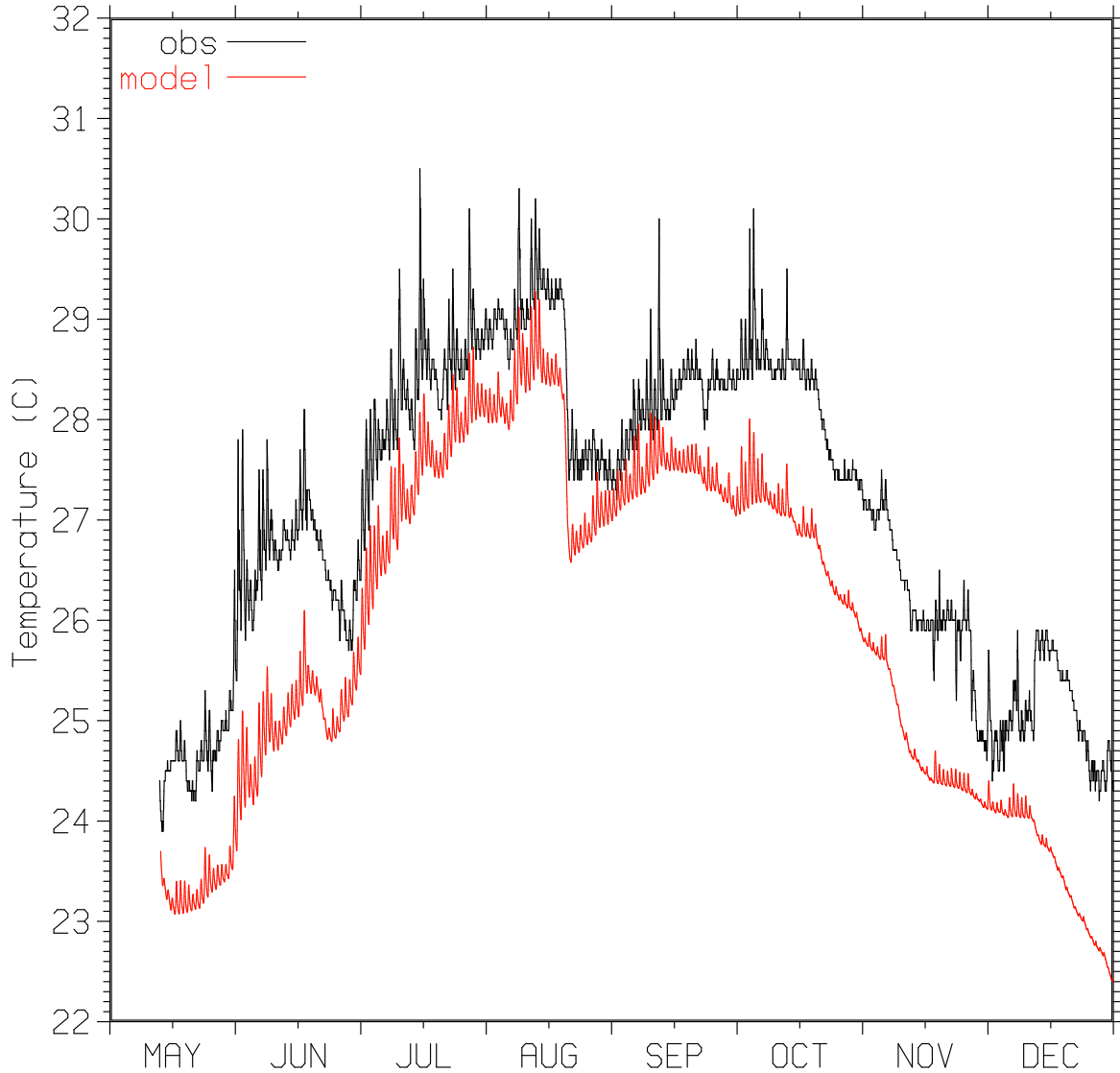
Fig. 17 — SST at Buoy 41049 for May through December 2009: observed (black), simulated with MYL2
MLM with reduced Qiao et al. (2004) wave mixing with $\alpha = 0.1$ (red)

Figure 17 shows the observed and simulated SST for a simulation at Buoy 41049 for May
through December 2009 conducted with the MYL2 MLM without the Large et al. (1994) mixing
enhancement and with the B_v wave mixing of Qiao et al. (2004) reduced by 90% ($\alpha = 0.1$).

With the reduced wave mixing, the seasonal variability of the simulated SST is larger than
that of the observed SST, i.e., the simulated SST increases more than the observed SST from May
through August. The SST spikes are larger than with the full B_v wave mixing in Fig. 16, but
most of the SST spikes are still smaller than those observed and those simulated without the wave
mixing in Fig. 15.

The magnitude of the simulated SST drop in August is in good agreement with the magnitude
of the observed drop. Since the contribution of the B_v wave mixing was substantially reduced for
this simulation, the increased drop in SST may be partly due to the increased stratification at the
base of the SML for this simulation due to the reduced mixing and shallower mixed layer.
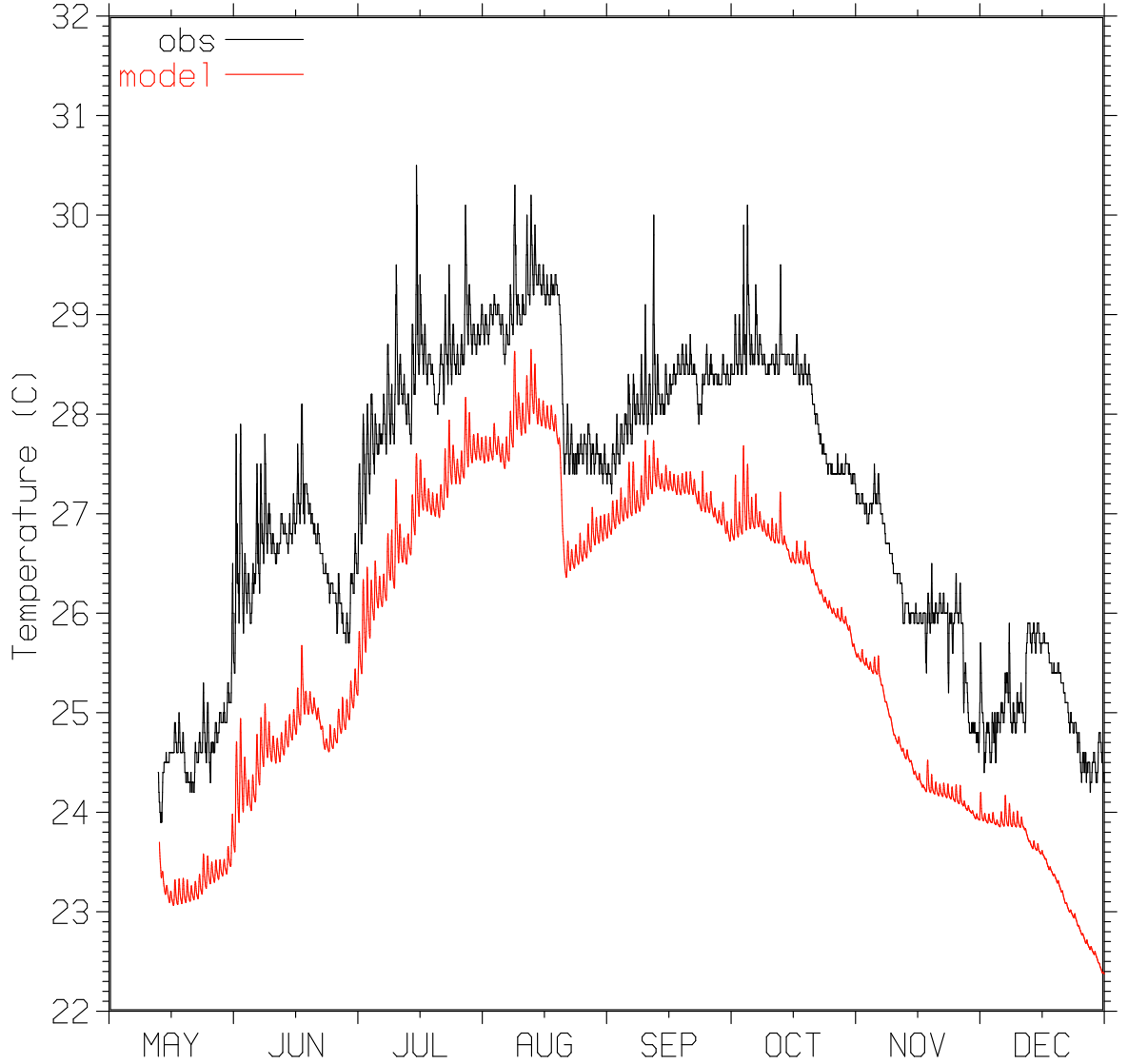
Fig. 18 — SST at Buoy 41049 for May through December 2009: observed (black), simulated with MYL2 MLM with reduced Qiao et al. (2004) wave mixing with $\alpha = 0.1$ and with Large et al. (1994) mixing enhancement (red)

To consider this further, the simulation with the reduced B_v wave mixing ($\alpha = 0.1$) was repeated with the Large et al. (1994) mixing enhancement added to increase the mixing. The SST from this simulation is shown in Fig. 18. The increased mixing results in less warming of the SST from May through August than in Fig. 17, and the SST drop in August is also reduced to about 1.6 °C and is just slightly greater than that in Fig. 15 with the Large et al. (1994) mixing enhancement and without the B_v wave mixing. Hence, the partial B_v wave mixing with $\alpha = 0.1$ reduces the magnitude of the SST spikes relative to the simulation without B_v wave mixing and slightly increases the mixing during the August wind event.

6. SUMMARY

The testing of the parameterization of direct wave mixing proposed by Qiao et al. (2004) with time-series observations from OWS Papa and from two NOAA buoys in the northeast Pacific

and from one NOAA buoy in the northwest Atlantic encountered two significant problems. At OWS Papa, the wave mixing caused too much diffusion of heat out of the SML and into the seasonal thermocline in the summer. This resulted in a loss of heat from the SML into the seasonal thermocline and too much diffusion (dispersion) of the seasonal thermocline itself.

At OWS Papa and at the NOAA buoys, the direct wave mixing inhibits the formation of very shallow mixed layers during calm or light-wind conditions and the associated SST spikes that occur because the surface heating is trapped within a shallow SML. There is some uncertainty about this result at Papa because of uncertainties in running a wave model at a single location to predict the local waves, i.e., a wave model run at a single location cannot properly account for waves and swell propagating towards that location from other areas. However, the observations from the NOAA buoys contain spectral wave data; hence, the wave mixing can be computed directly from the wave observations.

The wave observations from all three buoys indicate that the significant wave height during light-wind and calm conditions rarely drops below about 1 m, which is due mainly to swell propagating to the locations of the buoys from other areas. With the parameterization of direct wave mixing by Qiao et al. (2004), this swell is sufficient to generate enough mixing to prevent very shallow mixed layers and SST spikes from occurring.

A number of the direct wave-mixing papers discuss significant uncertainty regarding the magnitude of the proposed wave mixing, e.g., Eq. (1) from Qiao et al. (2004) contains the scaling factor α. Simulations at Papa and at the NOAA buoys, besides being run with the full wave mixing with $\alpha = 1$ as in Qiao et al. (2004), were run with $\alpha = 0.1$ to reduce the wave mixing by 90%. With the reduced wave mixing, the problem of too much diffusion of the seasonal and diurnal thermoclines is significantly reduced; however, the results indicate that even with a reduction of 90%, this diffusion is still too high.

Both of the problems with the direct wave mixing that were encountered can be associated with the fact that the B_v wave mixing profiles do not take any account of stratification. Hence, the B_v wave-mixing diffuses heat and other water properties through the diurnal and seasonal thermoclines, and diffuses the thermoclines as well.

7. ACKNOWLEDGMENTS

8. REFERENCES

Babanin, A.V. (2006). "On a Wave-induced Turbulence and a Wave-mixed Upper-ocean Layer," *Geophys. Res. Lett.* **33**, L20605, doi:10.1029/2006GL027308.

Babanin, A.V., A. Ganopolski, and W.R.C. Phillips (2009). "Wave-induced Upper-ocean Mixing in a Climate Model of Intermediate Complexity," *Ocean Modelling* **29**, 189–197.

Babanin, A.V. and B.K. Haus (2009). "On the Existence of Water Turbulence Induced by Non-Breaking Waves," *J. Phys. Oceanogr.* **39**, 2675–2679.

Barron, C.N., A.B. Kara, H.E. Hurlburt, C. Rowley, and L.F. Smedstad (2004). "Sea Surface Height Predictions from the Global Navy Coastal Ocean Model (NCOM) During 1998–2001," *J. Atmos. Oceanic Technol.* **21**(12), 1876–1894.

Berliand, T.G. (1960). "Climatological Method of Total Radiation," *Meteor. Gidrol.* **6**, 9–12.

Blumberg, A.F. and G.L. Mellor (1987). "A Description of a Three-dimensional Coastal Ocean Model," In *Three-Dimensional Coastal Ocean Models, Coastal Estuarine Stud.*, Vol. 4. N. Heaps, ed. (AGU, Washington, D.C.) pp. 1–16.

Dai, D., F. Qiao, W. Sulisz, L. Han, and A.V. Babanin (2010). "An Experiment on the Non-breaking, Surface-wave-induced, Vertical Mixing," *J. Phys. Oceanogr.* **40**, 2180–2188.

Davis, R.E., R. DeSzoeke, and P.P. Niiler (1981). "Variability in the Upper Ocean during MILE. Part1: The Heat and Momentum Balances," *Deep-Sea Res.* **28A**(12), 1427–1451.

Denman, K.L. and M. Miyake (1973). "Upper Layer Modification at Ocean Station Papa: Observations and Simulation," *J. Phys. Oceanogr.* **3**, 185–196.

Garratt, J. R. (1977). "Review of Drag Coefficients over Oceans and Continents," *Mon. Weather Rev.* **105**, 915–929.

Gaspar, P. (1988). "Modeling the Seasonal Cycle of the Upper Ocean," *J. Phys. Oceanogr.* **18**, 161–180.

Jerlov, N. G. (1968). *Optical Oceanography* (Elsevier Publ. Co., Inc., New York), 194 pp.

Jerlov, N. G. (1976). *Marine Optics* (Elsevier Publ. Co., Inc., Amsterdam), 231 pp.

Kantha L.H. and C.A. Clayson (1994). "An Improved Mixed Layer Model for Geophysical Applications," *J. Geophys. Res.* **99**, 25235–25266.

Large, W.G. (1996). "An Observational and Numerical Investigation of the Climatological Heat and Salt Balances at OWS Papa," *J. Climate* **9**, 1856–1876.

Large, W.G., J.C. McWilliams, and S. Doney (1994). "Oceanic Vertical Mixing: a Review and a Model with a Nonlocal Boundary Layer Parameterization," *Rev. Geophys.* **32**, 363–403.

Large, W.G. and S. Pond (1981). "Open Ocean Momentum Flux Measurements in Moderate to Strong Winds," *J. Phys. Oceanogr.* **11**, 324–336.

Levine, M.D., R.A. DeSzoeke, and P.P. Niiler (1983). "Internal Waves in the Upper Ocean during MILE," *J. Phys. Oceanogr.* **13**, 240–257.

Levitus, S. (1982). "Climatological Atlas of the World Ocean," NOAA Prof. Paper 13, U.S. Govt. Print Office, Washington, D.C., 173 pp.

List, R.J. (1958). *Smithsonian Meteorological Tables*, 6th ed. Publ 4014, Smithsonian Institution, Washington, D.C.

Liu, W.T., K.B. Katsaros, and J.A. Businger (1979). "Bulk Parameterization of Air-sea Exchanges of Heat and Vapor Including the Molecular Constraints at the Interface," *J. Atm. Sci.* **36**, 1722–1735.

Martin, P. J. (1985). "Simulation of the Mixed Layer at OWS N and P with Several Models," *J. Geophys. Res.* **90**, 903–916.

Martin, P. J. (1986). "Testing and Comparison of Several Mixed-Layer Models," NORDA Report 143. Naval Research Laboratory, Stennis Space Center, MS 39529, 30 pp.

Martin, P.J. (2000). "A Description of the Navy Coastal Ocean Model Version 1.0," NRL Report NRL/FR/7322–00-9962, Naval Research Laboratory, SSC, MS 39529, 42 pp.

Mellor, G.L. and P.A. Durbin (1975). "The Structure and Dynamics of the Ocean Surface Mixed Layer," *J. Phys. Oceanogr.* **5**, 718–728.

Mellor, G.L. and T. Yamada (1974). "A Hierarchy of Turbulence Closure Models for Planetary Boundary Layers," *J. Atmos. Sci.* **31**, 1791–1806.

Mellor, G.L. and T. Yamada (1982). "Development of a Turbulence Closure Model for Geophysical Fluid Problems," *Geophys. and Space Phys.* **20**, 851-875.

Morey, S.L., P.J. Martin, J.J. O'Brien, A.A. Wallcraft, and J. Zavala-Hidalgo (2003). "Export Pathways for River Discharged Fresh Water in the Northern Gulf of Mexico," *J. Geophys. Res.*, **108**, 1–15.

Qiao, F., Y. Yuan, Y. Yang, Q. Zheng, C. Xia, and J. Ma (2004). "Wave-induced Mixing in the Upper Ocean: Distribution and Application to a Global Ocean Circulation Model," *J. Geophys. Res. Lett.*, *31*, L11303, doi:10.1029/2004GL019824.

Reed, R.K. (1977). "On Estimating Insolation Over the Ocean," *J. Phys. Oceanogr.* **7**, 482–485.

Rogers, W.E., P.A. Hwang, and D.W. Wang (2003). "Investigation of Wave Growth and Decay in the SWAN Model: Three Regional-scale Applications," *J. Phys. Oceanogr.* **33**, 366–389.

Rutkovskaya, V.A. and E.N. Khalemskiy (1973). "Calculating the Depth of Penetration of Solar Enegy in Seawater (with the Pacific as an Example)," *Oceanology* **14**, 398–404.

Schiffer, R.A. and W.B. Rossow (1983). "The International Satellite Cloud Climatology Project (ISCCP): the First Project of the World Climate Research Programme," *Bull. Am. Meteor. Soc.* **64**(7), 779–784.

Tabata, S. (1964). "Insolation in Relation to Cloud Amount and Sun's Altitude," in *Studies on Oceanography*, Y. Kozo, ed. (University of Washington Press, Seattle), pp. 202–210.

Wyrtki, K. (1965). "The Average Annual Heat Balance of the North Pacific Ocean and its Relation to Ocean CircuLation," *J. Geophys. Res.* **70**, 4547–4559.

Yuan, Y., F. Qiao, F. Hua, and Z. Wan (1999). "The Development of a Coastal Circulation Numerical Model: 1. Wave-induced Mixing and Wave-current Interaction," *J. Hydrodyn.* Ser. A, **14**, 1–8.